Miner Deposita
DOI 10.1007/s00126-015-0610-3

ARTICLE

Hydrothermal remobilisation around a deformed and remobilised komatiite-hosted Ni-Cu-(PGE) deposit, Sarah's Find, Agnew Wiluna greenstone belt, Yilgarn Craton, Western Australia

Margaux Le Vaillant[1,2] · **Ahmad Saleem**[3] · **Stephen J. Barnes**[2] · **Marco L. Fiorentini**[1] · **John Miller**[1] · **Steve Beresford**[1] · **Caroline Perring**[4]

Received: 17 October 2014 / Accepted: 3 August 2015

Abstract The Sarah's Find nickel deposit, located 4.5 km north of the Mount Keith nickel mine, Western Australia, was chosen as a case study to investigate the nature and three-dimensional geometry of a geochemical halo created by the hydrothermal remobilisation of base metals and platinum group elements into the country rock surrounding a small massive Ni sulphide orebody. Portable and laboratory-based XRF analyses were carried out on samples from a shear zone localised along the basal komatiite-dacite contact that hosts the orebody. A geochemical halo was identified that extends along the shear zone up to 1780 m away from the massive sulphides, parallel to a prominent stretching lineation. Elevated Ni and Pd are associated with high As, Co, Cu and S. Palladium and Pt concentrations increase with proximity to massive sulphides (from 6 to 1190 ppb Pd). These anomalous concentrations reflect the presence of sulfarsenides and sulphides, either physically remobilised and forming veinlets close to the massive sulphides, or hydrothermally transported and redeposited within the foliation. In situ laser ablation ICP-MS indicates that Pd and Pt are hosted within these nickel sulfarsenides. This Ni-Co-As-Pd geochemical halo, observed around the Sarah's Find ore body, is interpreted as forming syn deformation, by the circulation of As-rich hydrothermal fluids dissolving base metals, Pd and Pt from the orebody and redepositing them along the sheared footwall contact. Similar Ni-Co-Pd-Pt-As geochemical haloes could potentially exist around any magmatic nickel sulphide mineral system that has undergone a phase of arsenic metasomatism and may be a generally applicable proximity indicator for nickel sulphides in hydrothermally altered terranes.

Keywords PGE · Komatiite · Western Australia · Metal remobilisation · Nickel sulphides · Hydrothermal halo · Arsenic

Introduction

The majority of magmatic nickel sulphide deposits have undergone post-emplacement deformation, metamorphism and metasomatism. The effect of deformation on these deposits, particularly tectonic modification of massive and disseminated sulphides, has been studied by numerous researchers (Bailey et al. 2006; Barnes et al. 1988; Barrett et al. 1977; Bleeker 1990; Collins et al. 2012; Cowden and Archibald 1987; Cowden and Roberts 1990; Duuring et al. 2007, 2010, 2012; Findlay 1998; Heath et al. 2001; Layton-Matthews et al. 2007; Seat et al. 2004; Vukmanovic et al. 2014). The effect of metamorphism and metasomatism on these deposits has been documented by Donaldson (1981), Barnes et al. (1988) and Goscombe et al. (2009), but there have been few studies looking at the effects of metamorphism and metasomatism on the composition of the country rocks and the possible

Editorial handling: R.L. Romer and G. Beaudoin

Electronic supplementary material The online version of this article (doi:10.1007/s00126-015-0610-3) contains supplementary material, which is available to authorized users.

✉ Margaux Le Vaillant
margaux.levaillant@csiro.au

[1] Centre for Exploration Targeting, School of Earth and Environment, Australian Research Council Centre of Excellence for Core to Crust Fluid Systems, The University of Western Australia, Perth, Australia

[2] CSIRO, Mineral Resources Flagship, Perth, Western, Australia

[3] School of Geosciences, Monash University, Melbourne, Australia

[4] BHP Billiton Nickel West, Perth, Australia

creation of a secondary hydrothermal halo around nickel sulphide deposits.

Elemental dispersion due to metasomatism of massive sulphides and remobilisation into the surrounding rocks has been postulated for some time, but little research has gone into determining the real nature of these haloes, their spatial extent, and whether or not they could be used as an effective exploration tool. A few studies, such as the work by Le Vaillant et al. (2015) at the Miitel deposit, Hanley and Bray (2009) at Sudbury (Canada), or Layton-Matthews et al. (2007) in the Thompson Nickel Belt (Canada), characterise hydrothermal remobilisation of nickel and/or other metals and platinum group elements (PGE) into the adjacent country rocks. Finally, a study by Barrie et al. (2007) explored the presence of hydrothermal halos around the River Valley, Ferguson Lake (Canada) and Kabanga (Tanzania) deposits. Their results highlight the presence of subtle anomalies in combined metal and/or transition elements in country rocks, extending up to several hundred meters away from massive sulphides.

The aim of this study was to evaluate whether a geochemical halo was formed around the Sarah's Find nickel deposit during metamorphism and/or hydrothermal alteration and, if present, determine its nature and extent. A structural study was first carried out to determine the structural architecture and provide a framework to constrain sample location and subsequent data interpretation. Geochemical analyses were then collected on targeted samples, using portable XRF and pre-existing exploration assay data as an initial screen for anomalous samples. Some of the samples containing anomalous results that could represent hydrothermal remobilisation of elements derived from the nickel sulphides were studied in more detail (SEM-EDS, XRF mapping, LA-ICP-MS) in order to identify mineral phases and their associations. Finally, all the results were interpreted using information on the structural setting and were plotted in a 3D model to determine the shape and extent of the observed halo.

Geological setting

Regional geology and deformation history

The Sarah's Find nickel deposit is located within the Mount Keith Domain, in the Agnew Wiluna Greenstone Belt (AWB) which occupies the northern part of the Norseman-Wiluna Greenstone Belt in Western Australia (Fiorentini et al. 2007) (Fig. 1). The AWB is part of the Kalgoorlie Terrane, located within the Eastern Goldfields Superterrane, in the eastern part of the Archaean Yilgarn Craton (Cassidy et al. 2006). The AWB is bounded to the west by the Waroona shear zone (Platt et al. 1978) and to the East by the Keith-Kilkenny tectonic zone (Eisenlohr 1988). The AWB is one of the most Ni-endowed belts in the world (Barnes and Fiorentini 2012a; Barnes et al. 2007; Hronsky and Schodde 2006) and hosts multiple nickel sulphide deposits such as Mount Keith, Perseverance and Rocky's Reward (Barnes 2006; Duuring et al. 2010, 2012; Fiorentini et al. 2010b). The AWB is composed of a narrow package of deformed and metamorphosed supracrustal rocks trending NNW-SSE and bordered by granitic gneiss terrains (Duuring et al. 2010; Eisenlohr 1988). This 2.7-Ga supracrustal sequence comprises felsic to intermediate volcanic and volcanoclastic rocks, sulphidic cherts, carbonaceous shales and laterally variable komatiites including cumulates, thin spinifex-textured units and komatiitic basalts (Fiorentini et al. 2007).

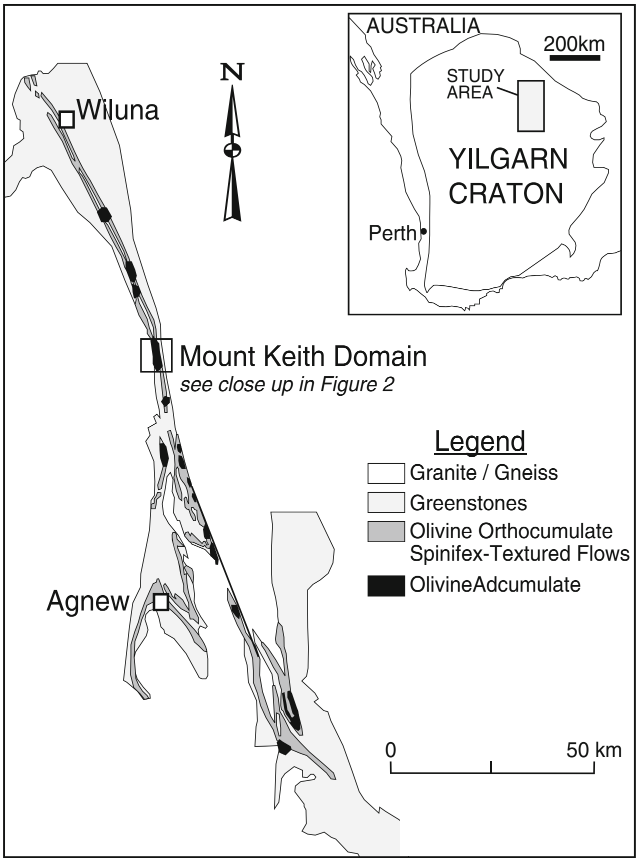

Fig. 1 Simplified geological map of the Agnew-Wiluna Greenstone Belt (AWB), Western Australia, modified from Barnes et al. (2011) and Fiorentini et al. (2007) after Hill and Gole (1990)

The Sarah's Find nickel deposit is located in the northern part of the Mount Keith Domain. The volcanological architecture of the Mount Keith Domain has been studied by many researchers over the years (Burt and Sheppy 1975; Dowling and Hill 1990; Hill et al. 1995; Rosengren et al. 2005, 2007). The Mount Keith Domain contains three ultramafic layers from bottom to top: (1) The Mount Keith Ultramafic unit (MKU), (2) the Cliffs Ultramafic unit (CLU) and (3) the Monument Ultramafic unit (MU). These three ultramafic horizons are separated by a variably deformed sequence of felsic and mafic rocks, ranging in composition from tholeiitic basalt to dacite. Rosengren (2004) divided the Mount Keith Ultramafic unit between the Mount Keith Complex and Sarah's Find into four sections referred to as pods and constrictions (Fig. 2). Sarah's Find is located north of pod 2 (Fig. 2), in the most attenuated portion of the Mount Keith Ultramafic Complex (~70 m wide), where crosscutting faults significantly disrupt the basal contact of the Mount Keith Ultramafic unit (Fiorentini et al. 2007).

The structural history of the East Yilgarn Craton has been addressed by Swager (1997) who summarised 10 years of prior research by many different authors (Archibald et al. 1978; Hammond and Nisbet 1992; Platt et al. 1978; Williams and Whitaker 1993). Blewett et al. (2010) presented a structural-event framework, based on another decade of research, incorporating six phases of deformation: (D1) ENE-WSW extension, (D2) ENE-WSW contraction, (D3) extension, (D4) (a and b) contraction and strike slip movement, (D5) NE-SW compression and dextral strike-slip and finally (D6) low strain vertical shortening. The D4b episode is interpreted as being the event during which most of the gold was deposited (Blewett et al. 2010). The Mount Keith Domain has undergone mid- to upper greenschist facies metamorphism (Barrett et al. 1977) and illustrates the entire deformation sequence as described by Swager (1997) and Blewett et al. (2010).

Geology and deformation history of the Sarah's Find deposit

The Sarah's Find nickel deposit is composed of very small lenses (1–2 m wide) or stringers (10–20 cm) of massive sulphides mostly located at the basal contact between the Mount Keith ultramafic unit and the Mount Keith dacite footwall. Few stringers of sulphides are also present within the footwall dacite (Fig. 3, long section BB′). The massive sulphides at Sarah's Find consist of a pyrrhotite-pentlandite assemblage with small (<5 %) and variable amounts of chalcopyrite. The Mount Keith Ultramafic unit is almost entirely composed of olivine cumulates, predominantly olivine adcumulates, rich in magnesium (Fo=92 to 94) (Barnes et al. 2011; Rosengren et al. 2007). Adcumulate-textured pods and lenses, particularly abundant in the thickest parts of the unit, are flanked by laterally extensive meso- and orthocumulate textured units. The massive sulphide lenses are overlain by laterally discontinuous pyroxenite and peridotite horizons (Brand 1993), and the upper portion of the peridotite unit (olivine orthocumulate) grades upward into a thin dunite layer (olivine adcumulate) that hosts pods of disseminated nickel sulphides (Fiorentini et al. 2007). A thin pyroxenitic layer is locally developed at the upper contact of the Mount Keith Ultramafic unit (Gole et al. 2013). Crosscutting faults significantly disrupt the basal

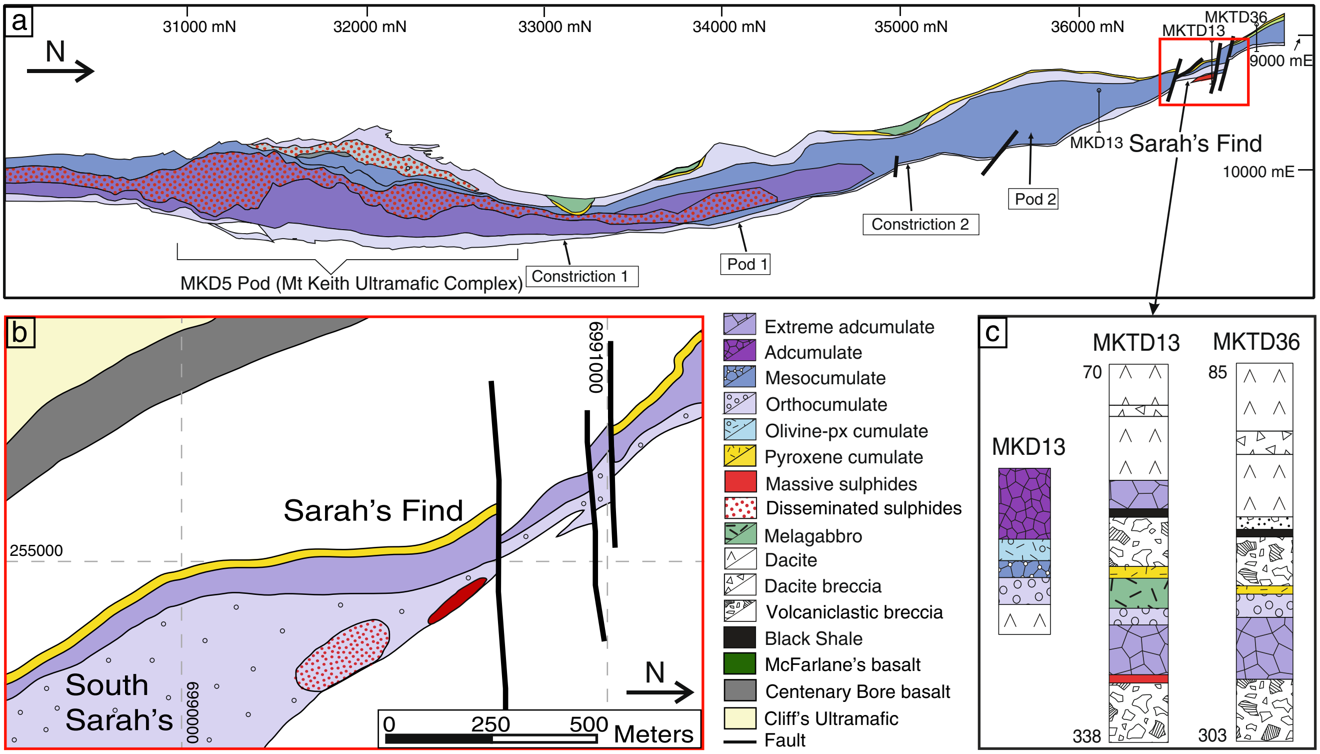

Fig. 2 **a** Detailed geology of the Mount Keith ultramafic complex (from Barnes et al. 2011; Fiorentini et al. 2007 after Rosengren et al. 2007); the *red box* indicates the location of the Sarah's Find deposit, and the location of the enlarged view of the geology presented in **b** illustrating the setting of the Sarah's Find massive and disseminated sulphides. **c** Drill holes logging of intersections of MKTD13, MKTD36 and MKD13 illustrating the stratigraphic sequence at Sarah's Find (from Rosengren et al. 2007 and Fiorentini et al. 2007)

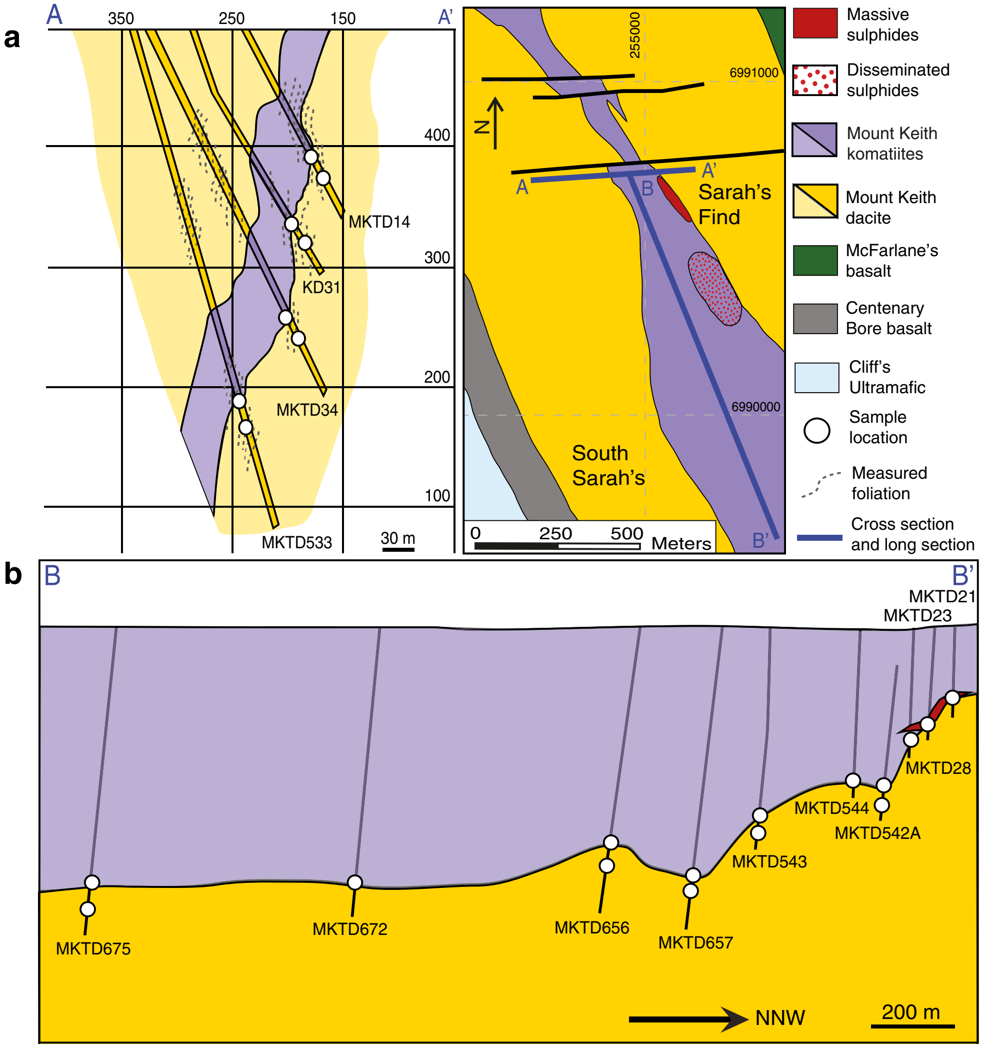

Fig. 3 **a** geological cross section (AA′) and **b** long section (BB′) through the Sarah's Find, illustrating the geometry of the system and indicating the location of studied drill holes (all the drill holes represented in the sections) and collected samples

contact of the Mount Keith Ultramafic unit which is entirely tectonic. The dacitic unit in the stratigraphic footwall has undergone polyphase deformation and alteration (Rosengren et al. 2008) including intense schistose to mylonite fabrics and alteration of the metamorphic minerals assemblage of quartz, sericite, chlorite, epidote (after plagioclase) and minor late crosscutting calcite veins (Fig. 4a–d). The footwall dacite is interpreted as a series of submarine lavas with associated volcaniclastic rocks (Rosengren et al. 2008).

Laboratory analyses were carried out on mineralised samples from the Sarah's Find massive sulphides (Table 1). The massive sulphide lenses at Sarah's Find, which are located at the contact with the footwall dacite, are relatively low in PGE compared to disseminated ores in the MKD5 ore body at Mount Keith and other komatiite-hosted nickel sulphide deposits (Barnes and Fiorentini 2012a), with average values of 139±74 ppb IPGE (Ir, Ru and Os) and 1179±1091 ppb PPGE (Pd, Pt, Rh and Au) (Fig. 5a, b). Platinum values within the ore show similar variations to other komatiite-hosted nickel sulphides (Fig. 5b), typically modelled as a consequence of variable silicate/sulphide mass ratio (R-factor) (Campbell and Naldrett 1979). However, Pd in the massive sulphides is very variable and does not follow expected R-factor trends (Fig. 5a). A similar observation can be made when studying the correlation between Pd and Pt (Fig. 5c). Finally, a good correlation is observed between Pd and As (Fig. 5d).

The structural history of the Sarah's Find deposit has not previously been studied in detailed. Hayward (2004) locally describes five stages of deformation at Mount Keith. $D1_{MK}$ and $D2_{MK}$ (where the suffix MK indicates that the terminology applies specifically to the Mount Keith areas, not to the belt as a whole) represent ENE-SWS shortening resulting in NNW upright folding ($D1_{MK}$) and the formation of reverse sinistral wrenches and faults ($D2_{MK}$). At Mount Keith, $D3_{MK}$ is characterised by minor recumbent folds, and $D4_{MK}$ produced NNE conjugate reverse faults and thrusts associated with the formation of most of the Yilgarn's gold. Finally, $D5_{MK}$ is characterised by NNE-trending dextral faults.

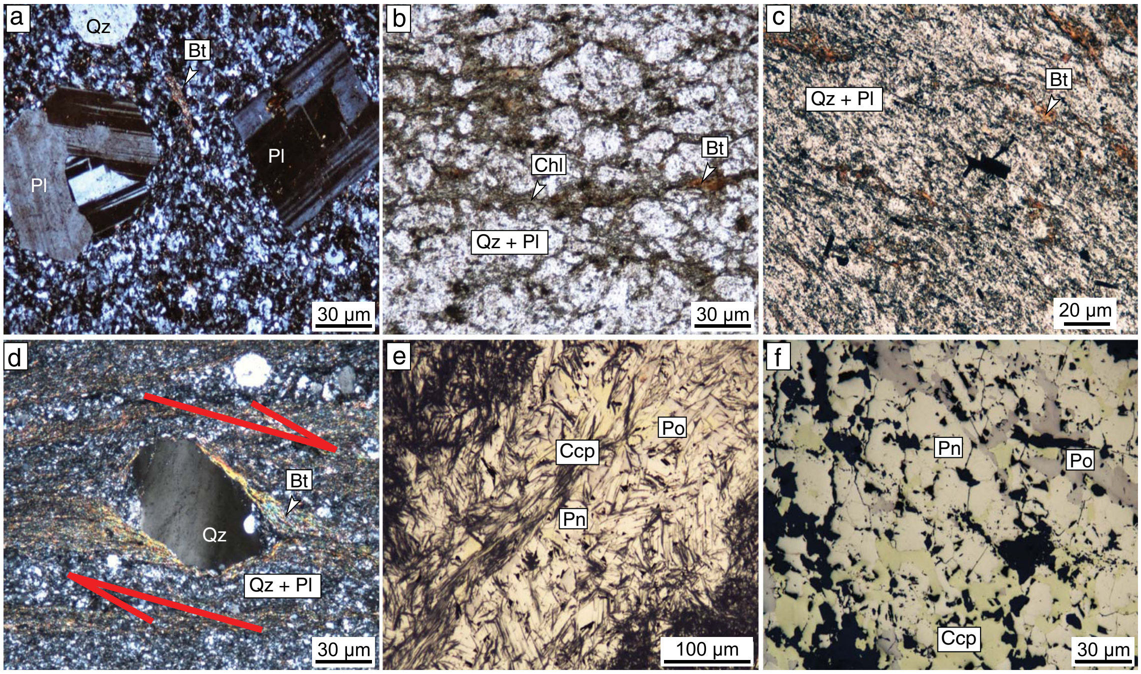

Fig. 4 Photomicrographs of the Mount Keith dacite and the massive sulphides at Sarah's Find illustrating typical facies. **a** Felsic porphyritic coherent unit of the footwall dacite with phenocrysts of quartz and plagioclase in a fine-grained matrix. **b** Weakly deformed Mount Keith dacite with little biotite alteration. **c** Strongly deformed and altered dacite, important biotite overprint. **d** Rotated quartz phenocryst with wrapping of the matrix and particularly of the biotite. **e** Deformed sulphides. **f** Typical massive sulphides composed of pyrrhotite, pentlandite and relatively abundant amounts of chalcopyrite

The results of our structural study show that the footwall contact at Sarah's Find is sheared and strongly altered to a chlorite-dominated assemblage and commonly obscured due to the presence of mafic dikes (Fig. 6, drill hole MKTD21). In the northern part of the deposit where massive sulphides are present, the footwall contact is undulating and steeply dipping (Fig. 6, drill hole MKTD21). Towards the south-west, the contact has a much shallower dip (Fig. 6, drill hole MKTD672).

The main massive sulphide bodies are located at the contact between the footwall dacite and the Mount Keith komatiites, where they have been sheared in a direction sub-parallel to the dominant foliation, itself folded into broad asymmetric folds. In some drill holes, this folding resulted in the apparent repetition of the massive sulphides (e.g. drill hole MKTD21, Fig. 6). Occasional very thin (10–20 cm thick) massive sulphide occurrences can also be found within the dacite, close to the footwall contact (drill holes MKTD23 and MKTD37). These thin sulphide lenses observed within the dacite footwall are in close proximity to the mineralised contact and are sub-parallel to the ductile fabric foliation.

The dominant foliation has a strike to the NNW, dipping to the WSW, but it can also trend NE, ENE and NW (Fig. 7a)—these variations are probably linked to large-scale flexures of the foliation caused by subsequent deformational events. The foliation has a strong mineral and stretching lineation defined by elongated plagioclase and quartz phenocrysts (Fig. 7c). Arsenopyrite grains, as well as other small sulphides, were observed to lie on foliation planes and to be elongated parallel to the stretching lineation (Fig. 7b). This lineation has a dominant rake shallowly to the SSE (mean of 26/ 175; Fig. 7g). Extensive kinematic markers indicate a dextral sense of shearing (Figs. 4d and 7e), for the current dominant SSW dip of the foliation and a small component of reverse movement. All measurements taken as part of the structural study are tabulated in Electronic Supplementary Materials (ESM) Table S1, along with a description of the methods used.

A set of late crosscutting dextral faults have been mapped regionally in the Mt Keith area (Hayward 2004). However, late-stage crosscutting faults were only occasionally observed in the drill core through the Sarah's Find deposit. In most areas, the transition between ultramafic and dacite units was within the ductile shear zone, with lithological contacts sub-parallel to the foliation. Brittle juxtaposition of the units was not commonly observed. There are minor occurrences of massive sulphides that are substantially off the main ultramafic–dacite footwall contact (drill holes MKTD544, MKTD543, MKTD619, MKTD21). These off contact sulphides transect the dominant foliation (Fig. 6d) and have been interpreted as being the product of late-stage remobilisation post-ductile shearing of massive sulphides.

Table 1 PGE and key chalcophile metals composition of massive and disseminated sulphide samples from the Sarah's Find deposit

Sample ID	Ni wt%	Cu wt%	Os ppb	Ir ppb	Ru ppb	Rh ppb	Pt ppb	Pd ppb	Au ppb	Pt + Pd ppb	IPGES Ir + Os + Ru	PPGES Pt + Pd + Rh + Au	As ppm	S wt%
2104	14.80	0.07	14	18	38	24	587	567	14	1154	70	1192	11	15.70
2108	8.59	0.23	32	51	84	64	201	71	13	272	167	349	6	22.70
2112	10.25	0.14	47	29	90	42	386	1115	24	1501	167	1566	1690	23.50
2301	7.49	0.12	38	24	90	38	692	2496	121	3188	152	3347	1130	10.30
2801	6.81	0.22	43	39	123	53	341	651	119	993	205	1165	823	23.60
53104	0.23	0.45	3	3	3	3	18	40	10	58	8	71	2	13.90
53407	10.48	0.16	39	36	131	50	277	146	91	424	206	565	237	25.10
AV	8.38	0.20	31	28	80	39	358	727	56	1084	139	1179	557	19.26
MD	8.59	0.16	38	29	90	42	341	567	24	993	167	1165	237	22.70
SD	4.45	0.12	16	16	46	20	228	871	52	1062	74	1091	670	5.84
ASD	53.12	62.46	53	55	57	52	64	120	93	98	53	93	120	30.31
Min	0.23	0.07	3	3	3	3	18	40	10	58	8	71	2	10.30
Max	14.80	0.45	47	51	131	64	692	2496	121	3188	206	3347	1690	25.10

All results are recalculated to a 100 wt% sulphides

Results

A major metasomatised zone was identified at Sarah's Find at the contact between the Mount Keith komatiites and the Mount Keith footwall dacite. Twenty-five drill holes crosscutting the footwall contact and spread over 2 km, going from the Sarah's Find massive sulphides (MKTD19, MKTD21 and MKTD14 crosscutting massive sulphides) to 1.5 km away from these massive sulphides (MKTD675), were selected for detailed relogging, structural study and sampling of the footwall contact area in order to detect the presence of a possible geochemical halo (Fig. 3). One hundred and twenty-six samples were collected and sent to Ultra Trace laboratories in Perth, Australia, for geochemical analyses, and 31 samples (from 17 different drill holes) were collected for portable XRF (pXRF) analyses.

Portable XRF and laboratory analyses

The concentrations of As, Ca, Cr, Cu, Fe, K, Mn, Ni, S, Si, Sr, Ti, Zn and Zr were determined by pXRF on lightly polished core surfaces for all the samples collected along the footwall contact. Analyses were collected following the analytical protocol from Le Vaillant et al. (2014) and described in ESM. The lithology associated with each analysis was determined using a Cr-Ti-Zr ternary diagram (Fig. 8, Hallberg 1984), allowing clear distinction between ultramafic rocks and felsic volcaniclastic lithologies. Results obtained with both laboratory analyses and pXRF show a tight cluster for the two lithologies. Moreover, analytical results for dacite samples at Sarah's Find correlate well with results from regional studies of dacite composition in the Eastern Goldfields Superterrane (Barley et al. 2008; Cassidy et al. 2006; Fig. 8). Results obtained from this regional dataset are used to evaluate background concentrations of Ni in the dacite footwall. For the purpose of this study, concentrations above 140 ppm, representing the 90th percentile on the nickel concentrations of the dacite across the craton (from the database of Barnes and Van-Kranendonk 2014), were considered as anomalous.

Both pXRF and laboratory XRF analyses on dacite samples from the Sarah's Find deposit yielded similar results (Fig. 9) (comparison study illustrated in ESM, Fig. S1 and Table S4; all pXRF and laboratory results are also tabulated in ESM Table S2c and Table S3a). Out of 80 dacite samples, 35 contain nickel concentrations above 150 ppm, with values ranging from 150 ppm to 1.2 wt% Ni. Within the pXRF analyses collected on dacite samples, seven analyses, collected on four different samples, show nickel values above 150 ppm, with values ranging from 245 to 2875 ppm Ni. These anomalous nickel concentrations are associated with elevated values in sulphur, copper and often arsenic (ESM Table S3b).

Analyses with elevated nickel concentrations are located either at the contact between the Mount Keith komatiites and the footwall dacite, or within 10 m of it. Six samples contain

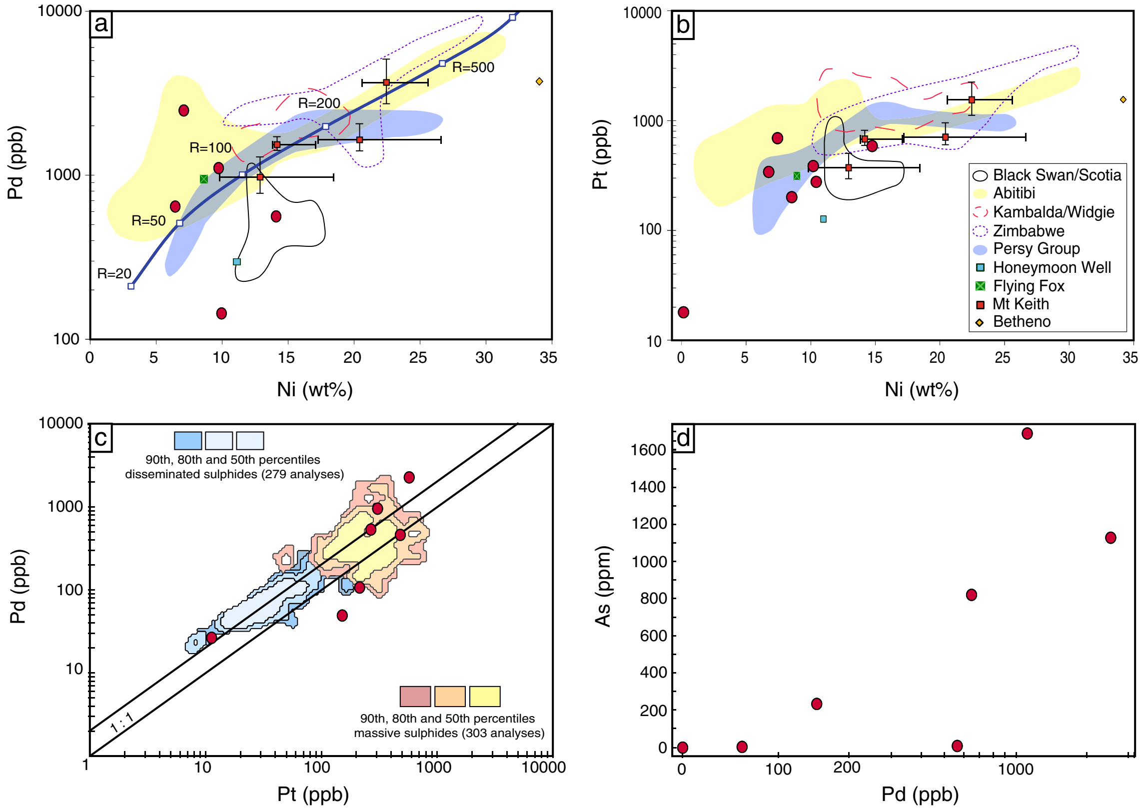

Fig. 5 Composition of Sarah's Find sulphides. **a**, **b** Pt, Pd and Ni expressed as element concentration in 100 % sulphide. **c**, **d** Pd, Pt and As expressed in ppb as element concentration recalculated to volatile free only. In **a**, the model curve shows the composition of magmatic sulphide component formed by bulk equilibration with komatiite magma of starting composition: 1600 ppm Ni, 10 ppb Pd, 1 ppb Ir, 30 wt% MgO, with a constant value of sulphide/silicate partition coefficient for Ni of 250 and 100 K for Pd, at different values of R-factor (indicated on frame). In plots **a** and **b** the data from other deposits is extracted from Barnes and Fiorenitni (2012a). In plot **c**, the 50th, 80th and 90th percentile contours were obtained using data from Barnes and Liu (2012b)

small amounts of nickel sulphides. The two samples with elevated Ni concentrations are MKTD23-302.65 and MKTD506-276.8. MKTD23-302.65 is located less than a meter away from massive sulphides, next to a thin sulphide stringer hosted by the dacite, close to the footwall contact (Fig. 10a). MKTD506-276.8 is located exactly on the footwall contact but over 50 m away from intersected massive sulphides. None of the other samples with nickel concentrations over 150 ppm contain visible nickel sulphides (Fig. 10b–e).

Forty-two of the dacite samples were also analysed for PGE. Figure 11 shows the results obtained for Pd, Pt and Ru. Twenty-five out of the 42 samples analysed have PGE concentrations below detection limit, but 12 contain Pd concentrations ranging from 6 to 3160 ppb. These high Pd concentrations also correspond to high Pt concentrations, ranging from 3 to 154 ppb, and correlate with high nickel concentrations (110 to 2875 ppm Ni). Interestingly, Pd is systematically more enriched than Pt, contrasting with usual magmatic proportions of 1 to 1 (ESM Table S3b).

Apart from a correlation between Na and K and a weak relationship between elevated Ni values and elevated Na, major element analyses in dacite do not show detectable systematic changes that were observed either in the variation of concentrations relative to the distance to the massive sulphides or in the combined variations of the various elements.

Mineralogy of the samples containing anomalous nickel concentrations (micro XRF mapping, SEM-EDS, 3D micro-tomography)

Four dacite samples that were identified as containing anomalous nickel concentrations were studied by micro-XRF mapping, SEM-EDS analyses, petrographic studies and electron microprobe analyses, in order to identify spatial relationship between nickel and other elements and to determine the mineral phase(s) hosting the nickel. Results of this study show that the anomalous nickel is mainly present as nickel sulfarsenides (gersdorffite NiAsS) and pentlandite ($[Ni,Fe]_8S_9$). Two types of settings and associations are observed:

1. The "Sulphide type" is composed of nickel sulphides and sulfarsenides, varying in size from 5 to over 150 μm diameter, associated with other sulphides (pyrrhotite, minor chalcopyrite and galena) and forming small sulphide stringers (Figs. 12 and 14a–c). These sulphide stringers do not follow the foliation.

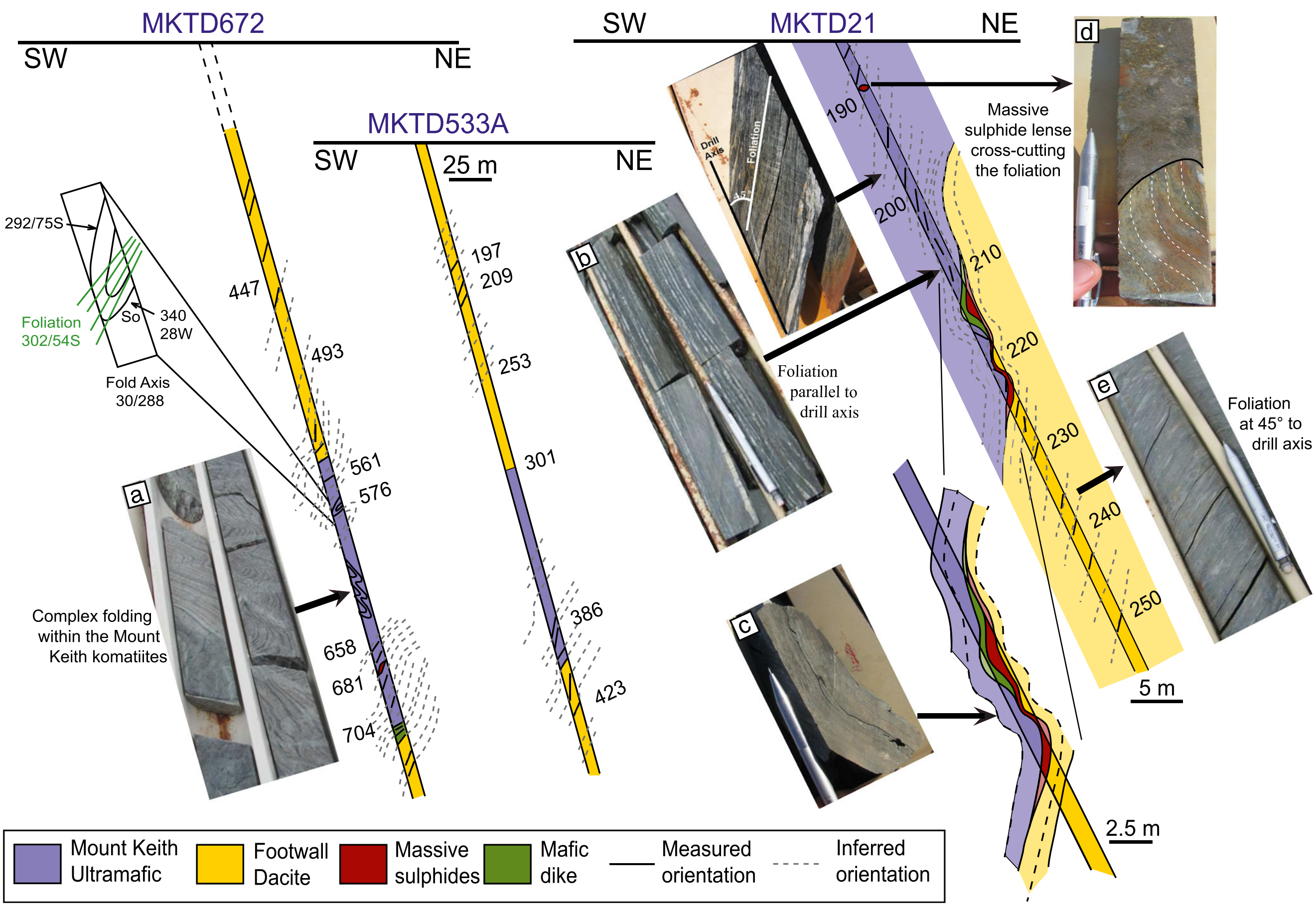

Fig. 6 Detailed structural logs of drill holes: MKTD21 intersecting the Sarah's Find massive sulphides, MKTD533A intersecting the barren footwall contact 90 m below the massive sulphides, and MKTD672 intersecting the footwall contact 1.5 km south of the Sarah's Find massive sulphides

2. The "foliation type" is composed of nickel sulphides and sulfarsenides, smaller in size, between a few microns to 50 µm in diameter, concentrated within the foliation, typically elongated along the lineation, and associated with

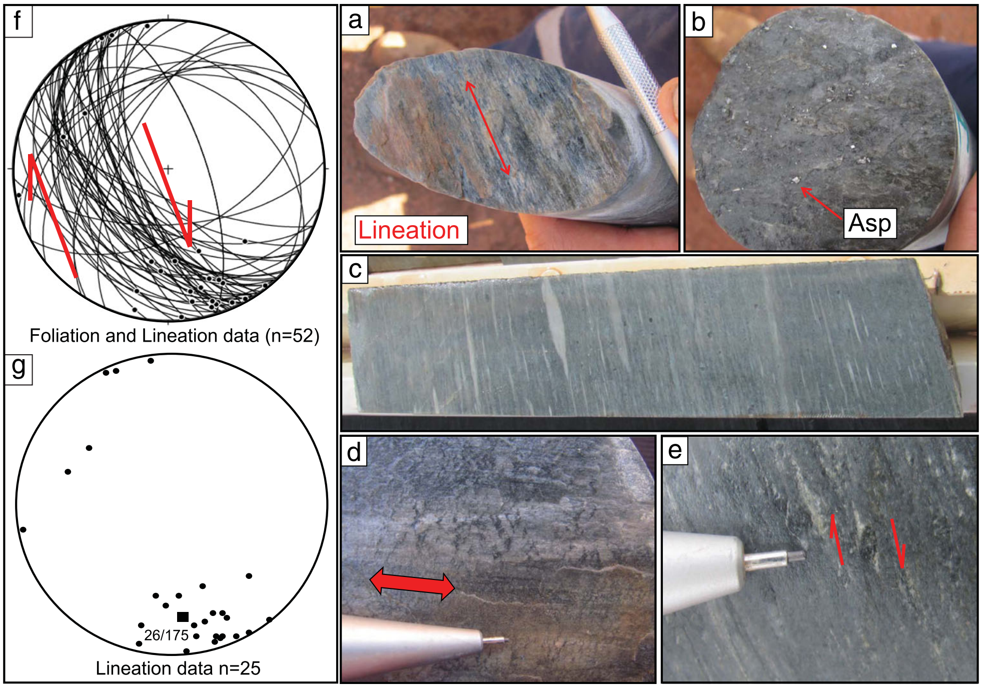

Fig. 7 Illustration of the various structures observed and measured within the Mount Keith footwall dacite. **a** Stretching lineation of the plagioclase phenocrysts, **b** arsenopyrite grains observed aligned along the foliation, **c**, **d** evidences of stretching and **e** rotated quartz phenocryst, dextral movement. **f**, **g** represent all the foliation and lineation measurement taken on the Mount Keith dacite. *Asp* Arsenopyrite

Fig. 8 Ternary diagram used to validate the rock identification and lithologies attributed to the various pXRF and laboratory analyses. The density contours were produced on data density plots for regional dacite with a dataset composed of 100 analyses of dacite samples from the Kalgoorlie South greenstone belt, the Agnew-Wiluna greenstone belt and the Kurnalpi greenstone belt (dataset from Barnes and Van-Kranendonk 2014)

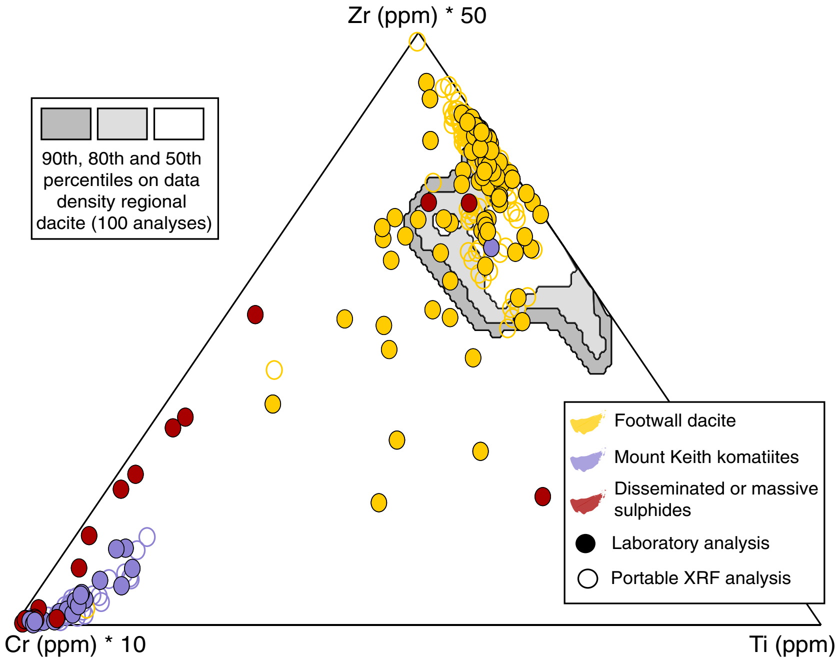

other small sulphides also concentrated within the foliation (pyrrhotite, minor pyrite and chalcopyrite, and rare sphalerite and galena) (Figs. 13 and 14d–f). In this second setting type, nickel sulfarsenides are dominant. The alignment of the sulphides and sulfarsenides along the foliation is shown in 2D and 3D in Fig. 13.

Mineral chemistry of the Ni-Co sulfarsenides

The Ni-Co sulfarsenides present in the footwall dacite in both the "sulphide" and "foliation" type occurrences were analysed by electron microprobe (details in ESM), highlighting the variations between the two types: (1) the small nickel sulfarsenides of the foliation type are cobalt-rich (27–31 wt%), nickel-poor (1.7–4 wt%) gersdorffites, whereas (2) the larger nickel arsenides of the sulphide type are generally more cobalt-poor (2–16.5 wt%), nickel-rich (12.6–24.6 wt%) gersdorffites (Fig. 15). Both types of gersdorffite can be found in the same sample such as in MKTD506-273 (Fig. 14b and c sulphide-associated type, d foliation-associated type). Within the sulphide type (nickel-rich gersdorffites), there are variations between Ni and Co compositions between the two samples (MKTD19-281 and MKTD506-273). In sample MKTD19-281, within the sulphide stringers, very close to the massive sulphides, both cobalt- and nickel-rich gersdorffites are present. In contrast, in sample MKTD506-273, the gersdorffites located further away from known massive sulphides (50 m) are nickel-rich/cobalt-poor. Foliation type gersdorffites are consistently Co rich, whereas sulphide type gersdorffites show more variable contents in Ni and Co.

In situ analyses for PGE by Laser Ablation ICP-MS of gersdorffites were collected at the University of Quebec in Chicoutimi (UQAC), Canada (details of the analytical protocol can be found in ESM, and all the results are tabulated in Table S5c). All the results are plotted in Fig. 16, as spider diagrams comparing the variations between the two gersdorffite types. IPGE are generally low, and their concentrations do not vary much between samples even though sulphide type gersdorffites show slightly higher concentrations. Combining all the analyses, concentrations of IPGE (Ir + Os + Ru) vary between 0.67 and 3.53 ppm. In contrast, PPGE (Pt + Pd) vary widely in composition between samples. Sulphide type gersdorffites contain higher concentrations of Pd with average values for the two samples of 11.8 and 350 ppm Pd, whereas foliation type gersdorffite show average concentrations between 0.99 and 1.8 ppm Pd. In contrast, Pd and Au concentrations are higher in the foliation type gersdorffites (average between 2.4 and 3.45 ppm Au) than the sulphide type ones (averages of 0.3 and 2.2 ppm Au). Platinum values are very low within foliation type gersdorffites (averages between 0.13 and 0.2 ppm Pt) and slightly higher within sulphide type ones (averages of 0.16 and 1.9 ppm Pt). However, Pt values are very heterogeneous within the analysed gersdorffites, and the study of the laser ablation spectra allows the interpretation of Pt being mostly located in small inclusions rather than in the lattice of the grains, in contrast to Pd. Several small PGE-rich inclusions were found within both gersdorffites types but especially in one sample (MKTD19-281) located very close to the massive nickel sulphides.

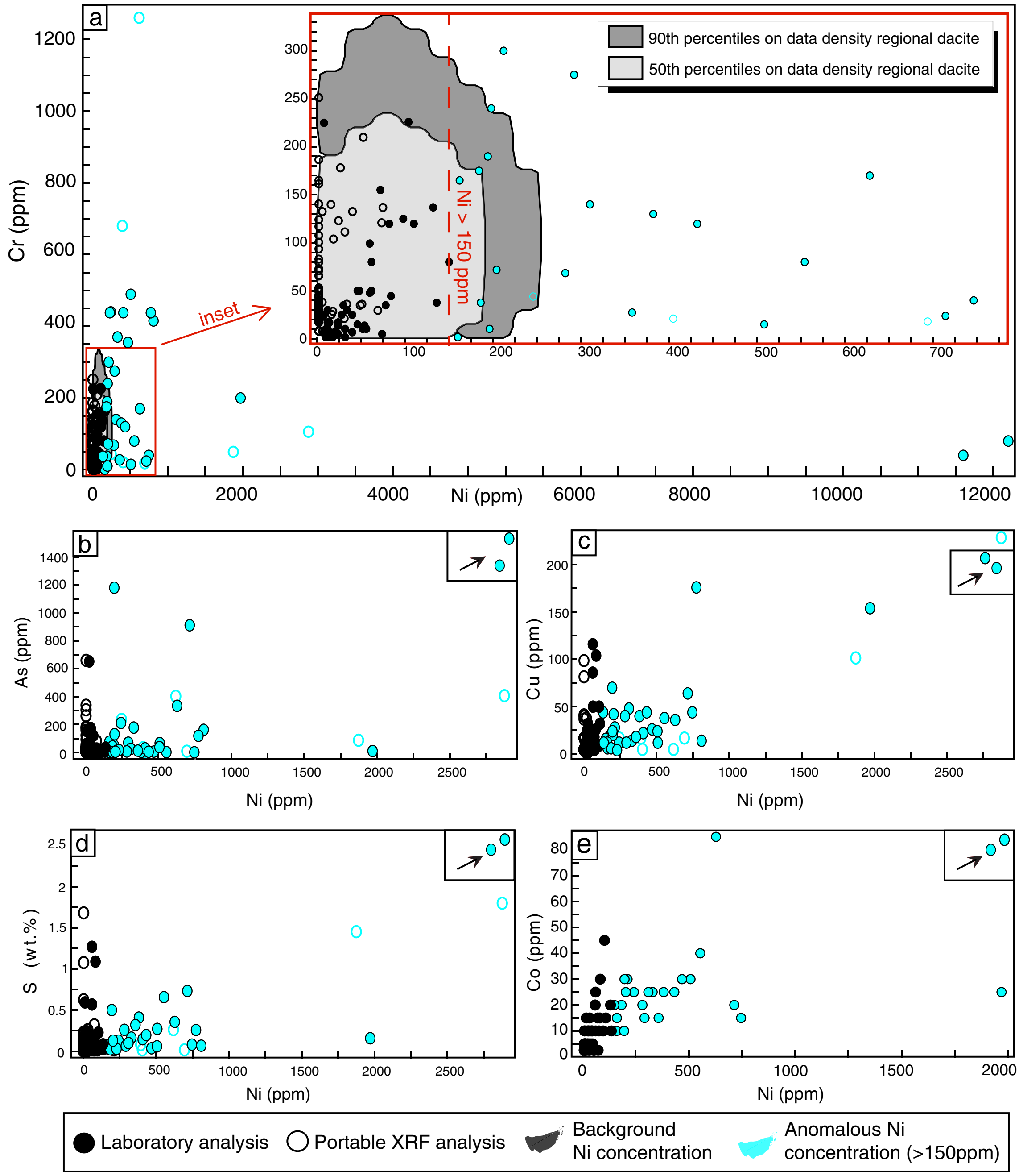

Fig. 9 Geochemical plots of Ni against various elements collected both by pXRF and laboratory analyses on Mount Keith dacite samples

Correlations between the various PGE concentrations were studied for the various samples (Table 2). Within MKTD19-281, located close to the massive sulphides and containing sulphide type gersdorffites, a strong correlation between Pd and Sb ($R_{\mathrm{Pd/Sb}}$=0.73) is observed; in contrast, Au is correlated with Pt ($R_{\mathrm{Au/Pt}}$=0.55) and with Sb ($R_{\mathrm{Pt,Au/Sb}}$=−0.56). Within MKTD506-273, which also contains sulphide type gersdorffites, a good correlation between the various IPGE is observed. Finally, within foliation type gersdorffites, two correlations are observed, between Pt and Os-Ir ($R_{\mathrm{Pt/Os}}$=0.72 and $R_{\mathrm{Pt/Ir}}$=0.51) as well as between Rh and Au ($R_{\mathrm{Rh/Au}}$=0.65).

3D data presentation

The results presented above establish the presence of associated anomalous concentrations of nickel, arsenic, palladium and cobalt within the footwall dacite, close to the footwall contact. To verify this association, a spatial relationship between the anomalous concentrations and the deposit scale arsenic metasomatism needed to be established. A 3D model was constructed, combining (1) the distribution of the arsenic at Sarah's Find with the structural measurements collected and (2) the location of geochemical samples exhibiting anomalous Ni, Co and Pd.

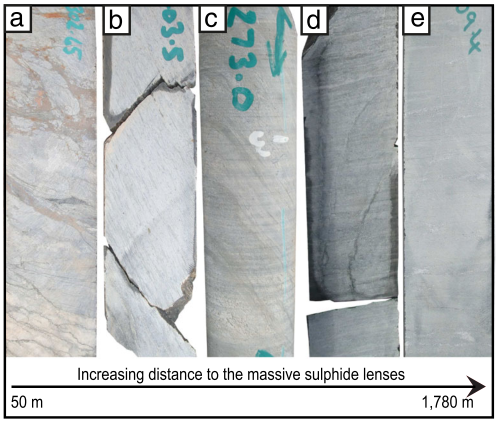

Fig. 10 Photomicrographs of dacite samples containing anomalous nickel concentrations

An interpolation of the arsenic concentrations was conducted using ordinary kriging (OK) and a structural trend corresponding to the measured foliation within the dacite footwall (foliation hosting arsenopyrite and nickel sulfarsenides grains, details on interpolation can be found in ESM). Arsenic concentrations are particularly elevated (As above 10 ppm) along the sheared footwall contact and close to the Sarah's Find massive sulphides (Fig. 17), with elevated arsenic concentrations extending into the footwall dacite. However, care must be taken when interpreting arsenic concentrations of the dacite footwall far from the footwall contact since assay sampling done by BHP Billiton is limited to less than 20 m after intersection of the footwall contact. Areas of elevated arsenic are also observed within the Mount Keith ultramafic unit, possibly indicating the presence of internal shearing. The spatial distribution of anomalous Ni, Pd and Co correlates well with the distribution of As (Fig. 17), and samples containing both anomalous arsenic and nickel (As> 10 ppm and Ni>150 ppm) are concentrated close to the massive sulphide lenses but also along the sheared footwall contact. Sample MKTD675-721 (Fig. 5), which contains 198 ppm Ni and 131 ppm As, is located on the sheared footwall contact and represents the dacite sample that was collected the farthest away, 1780 m, from the massive sulphide lenses. Interestingly, samples containing anomalous nickel concentrations (above 150 ppm) but arsenic below 10 ppm are usually located less than 40 m away from the Sarah's Find massive sulphides.

Discussion

This study has documented the presence of anomalous concentrations of Ni, Pd, Pt and Co within the footwall dacite, notably along the footwall contact. These anomalies extend up to 1780 m away from the massive sulphides. Detailed study of anomalous footwall dacite samples shows that elevated Ni, Pd and Co are associated with the presence of either tiny sulphide stringers containing pyrrhotite, pentlandite, gersdorffite and minor chalcopyrite and galena, referred to as the sulphide type, or with the presence of small gersdorffites and sulphide grains (mainly pyrrhotite, minor pentlandite, chalcopyrite, galena) lying

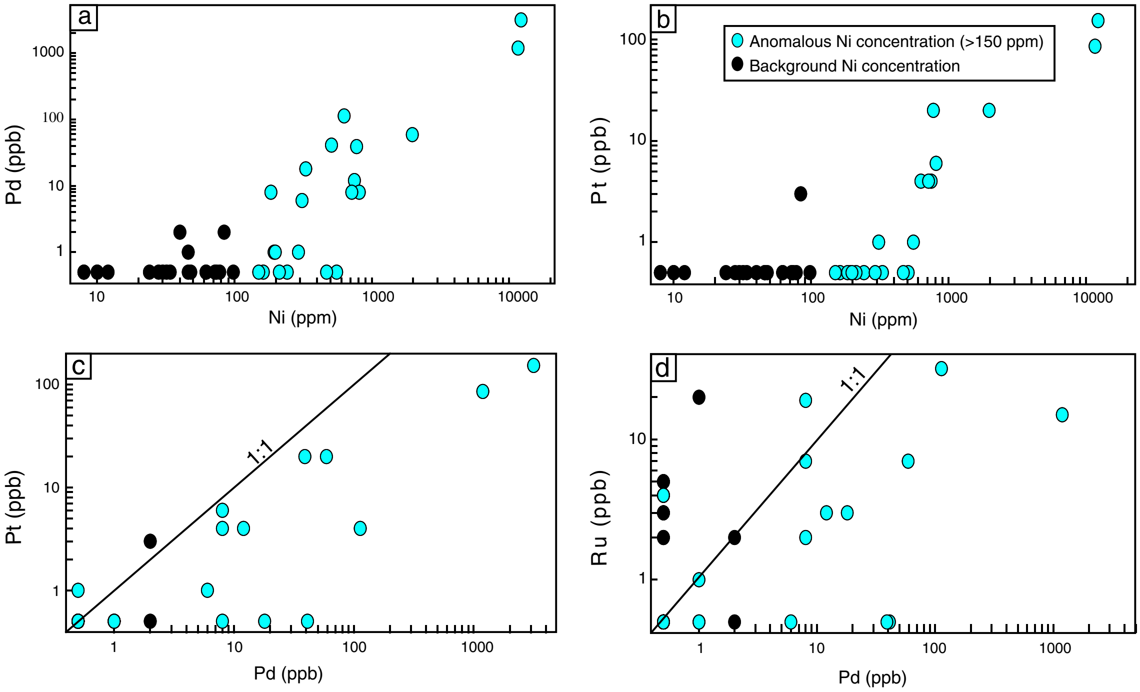

Fig. 11 Geochemical plot showing the variable degrees of correlation between the various platinum group elements and nickel for Mount Keith dacite samples

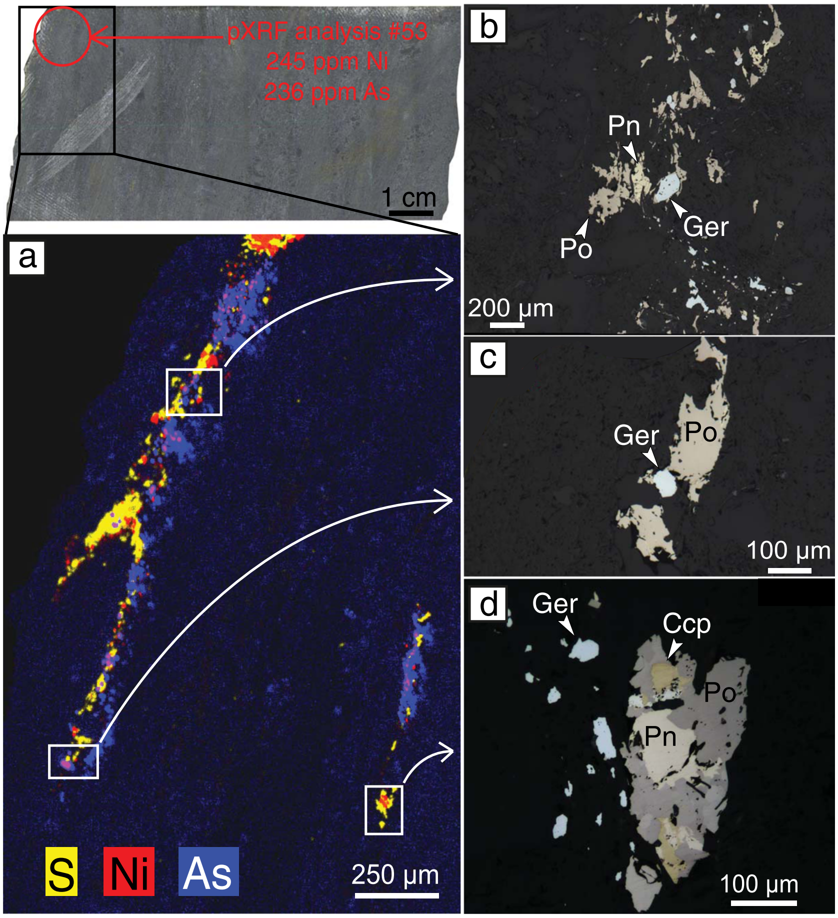

Fig. 12 Detailed study of sample MKTD560-273 showing anomalous concentrations of Ni, As, Co and Pd. **a** Three elemental (Ni, As, S) map obtained by micro-XRF mapping. **b**–**d** are petrographic reflected light photomicrographs of MKTD506-273. *Ccp* chalcopyrite, *Ger* gersdorffite, *Pn* pentlendite, *Po* pyrrhotite

along the foliation planes, referred to as the foliation type. The spatial study of Ni, Pd, Co and As concentrations emphasises the presence of these two types of association and their spatial occurrences. The high Ni concentrations observed close to the massive sulphides lenses are not necessarily associated with very elevated arsenic and can be related to the presence of sulphides and sulfarsenides associated with both the sulphide and foliation type occurrences close to the massive sulphides. In contrast, the high Ni concentrations systematically associated with elevated As are located along the sheared footwall contact, up to 1780 m away from the sulphides, and are associated with the foliation type occurrence.

The presence of these sulphide and sulfarsenides (of both sulphide and foliation type) within the footwall dacite is interpreted as being the result of the combined action of physical and hydrothermal remobilisation of the Sarah's Find massive sulphides. Sulphides present as very thin lenses within the dacite close to the footwall contact, and sulphides and sulfarsenides present in micro-scale stringer veins (sulphide type), where a clear association between sulphides and nickel sulfarsenides can be made, are interpreted as being the product of physical remobilisation of the massive sulphides. Within the foliation type occurrence on the other hand, most of the nickel is contained within nickel sulfarsenides, which are not associated with nickel sulphides; the anomalous nickel cannot be accounted for by physical remobilisation of the massive sulphides. Foliation type nickel sulfarsenides are interpreted as being the product of hydrothermal remobilisation of nickel by arsenic-rich hydrothermal fluids.

The observed elevated Ni and Co concentrations are also associated with anomalous Pd concentrations. In situ LA-ICP-MS analyses of both sulphide and foliation types nickel sulfarsenides indicate the presence of Pd in solid solution within the lattice of the grains. Palladium concentrations (as well as Pt concentrations) vary between the two different types of nickel sulfarsenides, with more elevated values observed for sulphide type sulfarsenides compared to foliation type sulfarsenides. However, Pd values, as well as Pt values, which are generally much lower, vary significantly between the different analysed samples. These variations are interpreted as small-scale, local variations of rock composition, fluid flow and fluid chemistry. Anomalous Pd values associated with Ni, Co and As in dacite samples collected along the sheared footwall contact and close to the massive sulphides are attributed to the presence of Pd within the sulfarsenides.

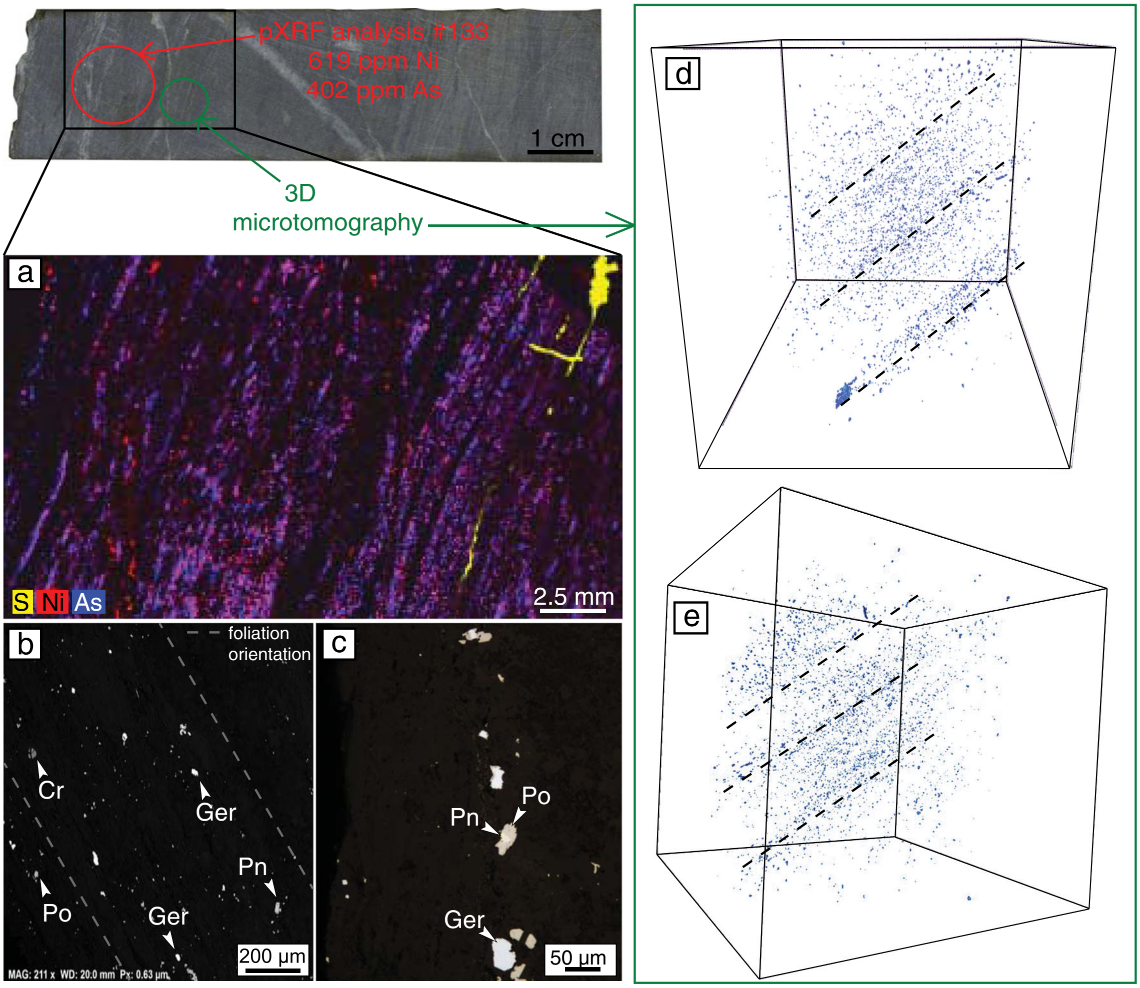

Fig. 13 Micro-XRF elemental map (**a**), petrographic reflected light photomicrographs (**b**, **c**) and snapshot of the 3D microtomograph of sample MKTD23-303 (**d**, **e**). *Ccp* chalcopyrite, *Ger* gersdorffite, *Pn* pentlendite, *Po* pyrrhotite

Source of Ni, Co and Pd

For the sulphide type gersdorffites, the source is interpreted to be small lenses of massive sulphides which have been physically remobilised into the footwall dacite. For the foliation type gersdorffites, the source is not as obvious. There are three possible sources for the anomalous Ni and Co concentrations detected where foliation type gersdorffites are present: (1) derivation from deep or distal sources on regional scale via the hydrothermal fluids, (2) the massive nickel sulphides and (3) the Mount Keith komatiites.

The arsenic metasomatism observed around the Sarah's Find prospect and within the footwall dacite has a larger extent than the observed Ni-Pd-Co halo, and multiple dacite samples show high As but no anomalous Ni and Co. If the arsenic-rich hydrothermal fluids are the medium that created the Ni- Co halo around the Sarah's Find deposit, this absence of anomalous Ni and Co in arsenic enriched dacite samples argues against the distally derived As-rich hydrothermal fluids being the source of the anomalous nickel.

The two possible remaining sources for the Ni and Co are the Mount Keith komatiites and the massive sulphides. The distinguishing characteristic of the massive nickel sulphides compared to the host ultramafic rocks is their enrichment in PGE. The unmineralised Mount Keith ultramafic unit is composed of olivine cumulates, which would be expected to contain no more than 2 ppb each of Pt and Pd (Fiorentini et al. 2010a). The Sarah's Find massive sulphides have average PGE concentrations, in a 100 % sulphides, of 167±74 ppb (median± SD) combined IPGE (Ir + Os + Ru) and 1165±1,091 ppb combined PPGE (Pd + Pt + Rh). The results of LA-ICP-MS analyses of the gersdorffites demonstrate the presence of Pd within them. Moreover, a good spatial association between high Pd concentrations and anomalous nickel concentrations is observed within the footwall dacite especially close to the footwall contact. These observations confirm that the Ni and Pd were probably remobilised together. On this basis and given the spatial association of the Ni-As-PGE anomalism with proximity

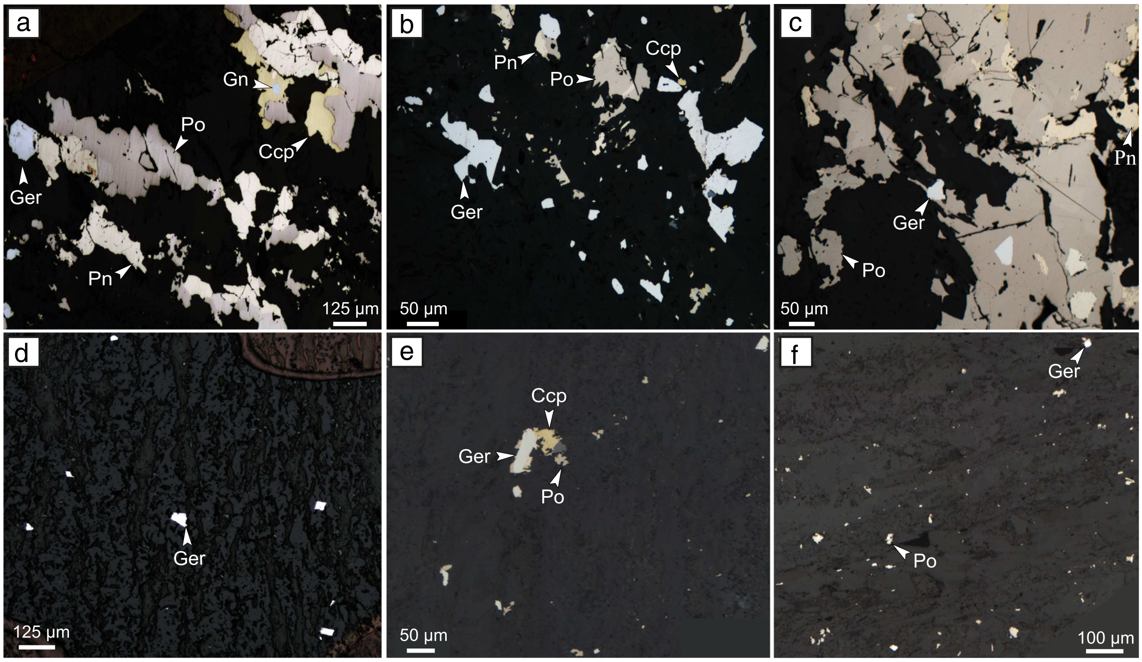

Fig. 14 Reflected light photomicrographs. **a**–**c** represent typical mineral associations and textures observed in samples containing sulphide-associated nickel sulfarsenides, whereas **d**–**f** represent typical mineral associations and textures observed in samples containing foliation-associated nickel sulfarsenides. **a** Sample MKTD19-281A, **b** sample MKTD506-273A, **c** sample MKTD506-273B, **d** sample MKTD506-273C, **e** sample MKTD23-303A and **f** sample MKTD23-303C. *Ccp* chalcopyrite, *Ger* gersdorffite, *Pn* pentlendite, *Po* pyrrhotite

to the ores and absence of this anomalism in the more distal samples, it is concluded that the Sarah's Find massive sulphides are the most likely source of Ni, Co and Pd, with the arsenic being derived from regional hydrothermal fluids.

Geometry of the hydrothermal halo

The geochemical Ni-Co-Pd-As halo observed around the Sarah's Find massive sulphides is interpreted as being the results of small-scale physical remobilisation of the massive sulphides as well as larger scale hydrothermal remobilisation of Ni, Co and Pd from the massive sulphides along the sheared footwall contact extending up to 1780 m away. Three-dimensional visualisation of the geochemical results and of the As distribution in the system supports this interpretation. Arsenic is elevated especially in close contact to the massive sulphides, which are an ideal source of S, Ni and Fe to form gersdorffite. The As-rich hydrothermal fluids are interpreted as circulating along the sheared footwall contact, since elevated arsenic concentrations are located along it. Moreover, since the gersdorffites deposited by these As-rich fluids are concentrated within the foliation and elongated along the measured mineral and stretching lineations (Fig. 12d, e), circulation through the system can be interpreted as being synchronous with the deformation that was responsible for the dominant foliation observed at Sarah's Find. Anomalous gold present in the arsenic-rich samples (12 to 230 ppb) and in the nickel sulfarsenides (0.01 to 421 ppm) suggests that these As-rich fluids are most likely associated with fluids associated with orogenic gold systems (Hedenquist et al. 2005).

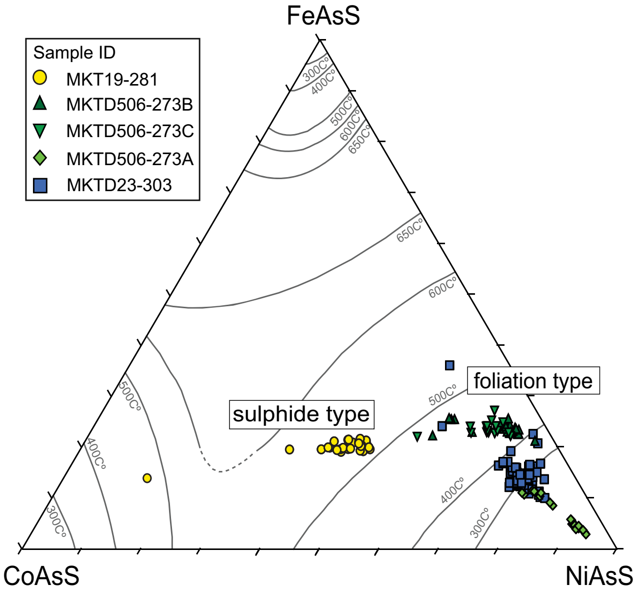

Fig. 15 CoAsS-FeAsS-NiAsS ternary diagram (mol %) showing the major elemental composition of both sulphide type and foliation type nickel sulfarsenides from the Sarah's Find deposit. The isotherms represent the upper limits of immiscibility (two phase fields) at various temperatures (after Klemm 1965)

Fig. 16 Spider diagrams showing the PGE compositions obtained by Laser Ablation ICP-MS for the various nickel arsenide types, as well as the few PGE-rich inclusions observed within these nickel-arsenides, in three different samples (MKTD19-281, MKTD506-273 and MKTD23-303)

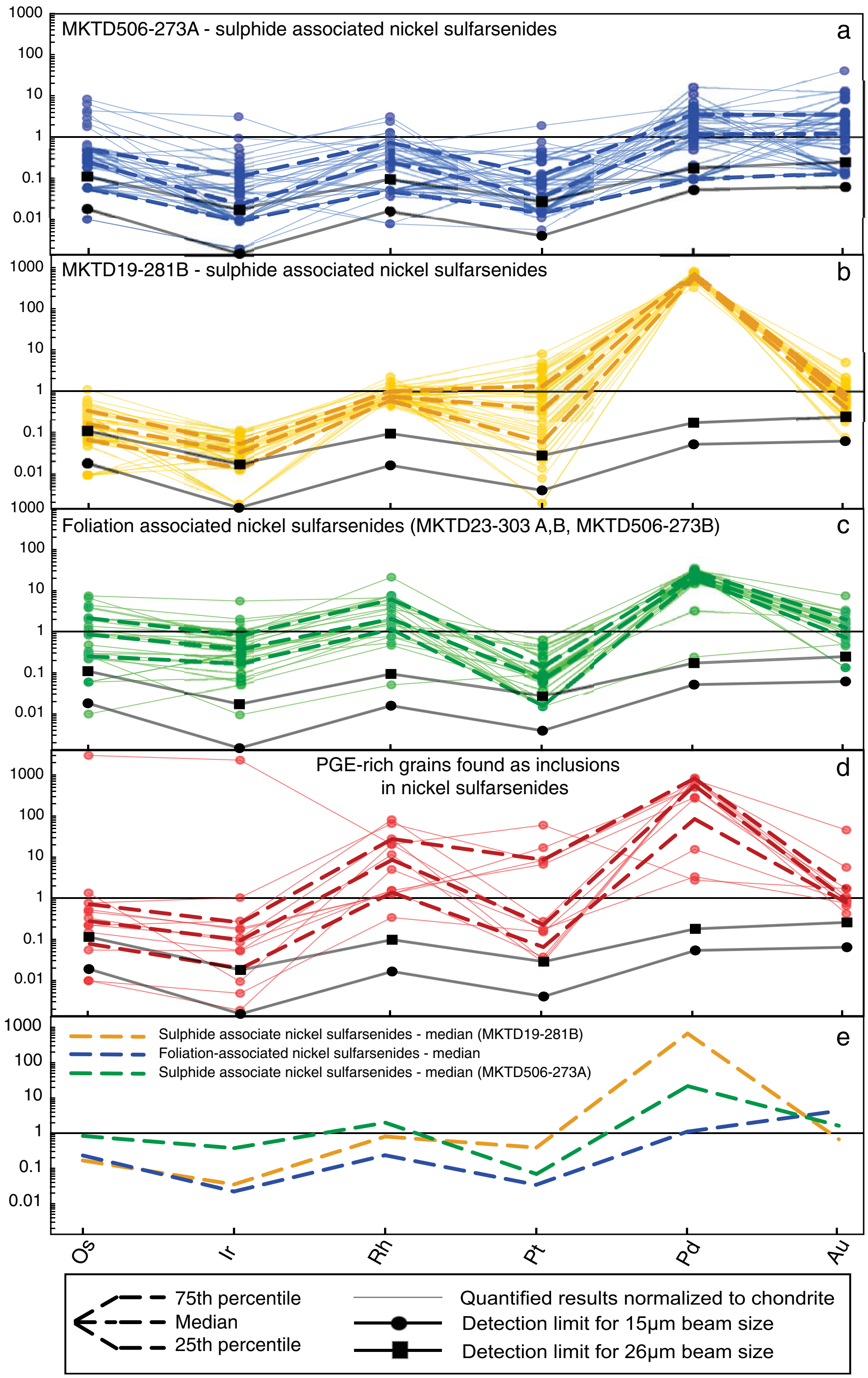

Source of the arsenic

The arsenic-rich fluids that circulated through the system could be associated with the regional orogenic gold event that Groves et al. (2003) linked with the circulation of crustal fluids. However, few crustal rock types can represent a realistic source of arsenic. Boyle and Jonasson (1973) studied the global distribution of arsenic and its abundance

Table 2 Correlations between the various PGE concentrations within these nickel sulfarsenides

"foliation-associated" arsenides (n= 45)

	Pd	**Pt**	**Rh**	**Ru**	**Os**	**Ir**	**Sb**	**Au**	**As**
Pd	1	0.06	0.57	-0.18	0.22	0.10	-0.06	0.20	-0.01
Pt	0.06	1	-0.08	-0.14	0.72	0.51	0.18	-0.11	0.23
Rh	0.57	-0.08	1	-0.24	0.35	0.10	-0.13	0.65	0.21
Ru	-0.18	-0.14	-0.24	1	-0.14	-0.10	-0.25	-0.06	-0.57
Os	0.22	0.72	0.35	-0.14	1	0.52	0.07	0.45	0.38
Ir	0.10	0.51	0.10	-0.10	0.52	1	0.19	0.02	0.17
Sb	-0.06	0.18	-0.13	-0.25	0.07	0.19	1	-0.15	0.44
Au	0.20	-0.11	0.65	-0.06	0.45	0.02	-0.15	1	0.34
As	-0.01	0.23	0.21	-0.57	0.38	0.17	0.44	0.34	1

"sulphide-associated" arsenides - sample MKTD19-281 (n= 38)

	Pd	**Pt**	**Rh**	**Ru**	**Os**	**Ir**	**Sb**	**Au**	**As**
Pd	1	-0.38	0.38	0.41	0.02	0.01	0.73	-0.27	0.82
Pt	-0.38	1	0.19	-0.05	-0.06	0.01	-0.56	0.55	-0.17
Rh	0.38	0.19	1	0.31	0.01	0.24	0.22	0.22	0.34
Ru	0.41	-0.05	0.31	1	0.41	0.38	0.35	0.10	0.36
Os	0.02	-0.06	0.01	0.41	1	0.39	0.01	-0.10	-0.08
Ir	0.01	0.01	0.24	0.38	0.39	1	-0.09	0.00	-0.12
Sb	0.73	-0.56	0.22	0.35	0.01	-0.09	1	-0.24	0.61
Au	-0.27	0.55	0.22	0.10	-0.10	0.00	-0.24	1	-0.11
As	0.82	-0.17	0.34	0.36	-0.08	-0.12	0.61	-0.11	1

"sulphide-associated" arsenides - sample MKTD506-273A (n= 27)

	Pd	**Pt**	**Rh**	**Ru**	**Os**	**Ir**	**Sb**	**Au**	**As**
Pd	1	0.22	0.45	-0.07	0.40	0.24	-0.14	0.13	0.38
Pt	0.22	1	0.03	-0.21	0.28	-0.06	0.06	0.49	0.13
Rh	0.45	0.03	1	0.19	0.54	0.33	0.05	0.00	-0.02
Ru	-0.07	-0.21	0.19	1	0.35	0.60	-0.58	-0.08	-0.66
Os	0.40	0.28	0.54	0.35	1	0.75	0.02	0.49	0.13
Ir	0.24	-0.06	0.33	0.60	0.75	1	-0.23	0.06	-0.07
Sb	-0.14	0.06	0.05	-0.58	0.02	-0.23	1	0.24	0.61
Au	0.13	0.49	0.00	-0.08	0.49	0.06	0.24	1	0.22
As	0.38	0.13	-0.02	-0.66	0.13	-0.07	0.61	0.22	1

in various rock types. The most endowed source of arsenic in the regional setting where the Sarah' Find deposit is located would be the black shales present in the country rocks. Samples from the Cobalt area, Ontario, of a similar Archaean lithology, yielded an average concentration of 80 ppm As (Boyle and Jonasson 1973). Furthermore, later studies by Quinby-Hunt et al. (1989) and Ketris and Yudovich (2009), on the world wide composition of shales, yielded average concentrations of 29 and 30 ppm As for carbonaceous shales, representing about 16 times the normal crustal average of 1 to 4 ppm As only (Large et al. 2011). Therefore, at Sarah's Find, there is enough crustal arsenic available to produce the arsenic-rich hydrothermal fluids responsible for the observed halo.

Practical application to exploration

The first step in using this Ni-Co-Pd-As geochemical halo as an exploration tool is the collection of Ni, Co and As assays in country rocks along contacts and major structures, instead of the normal practice of analysing these elements in ultramafic rocks only. Combined with a good understanding of the structural controls (faults, folds and foliation) and background composition of As, Ni, Co of the various country rock lithologies, this dataset can be used to produce a 3D model of the Ni, Co and As halo around massive nickel sulphides. With this 3D model, targets can be prioritised: High As, Ni and/or Co would be higher prospectivity area and high As but low Ni and/or Co being lower prospectivity areas. At Sarah's Find,

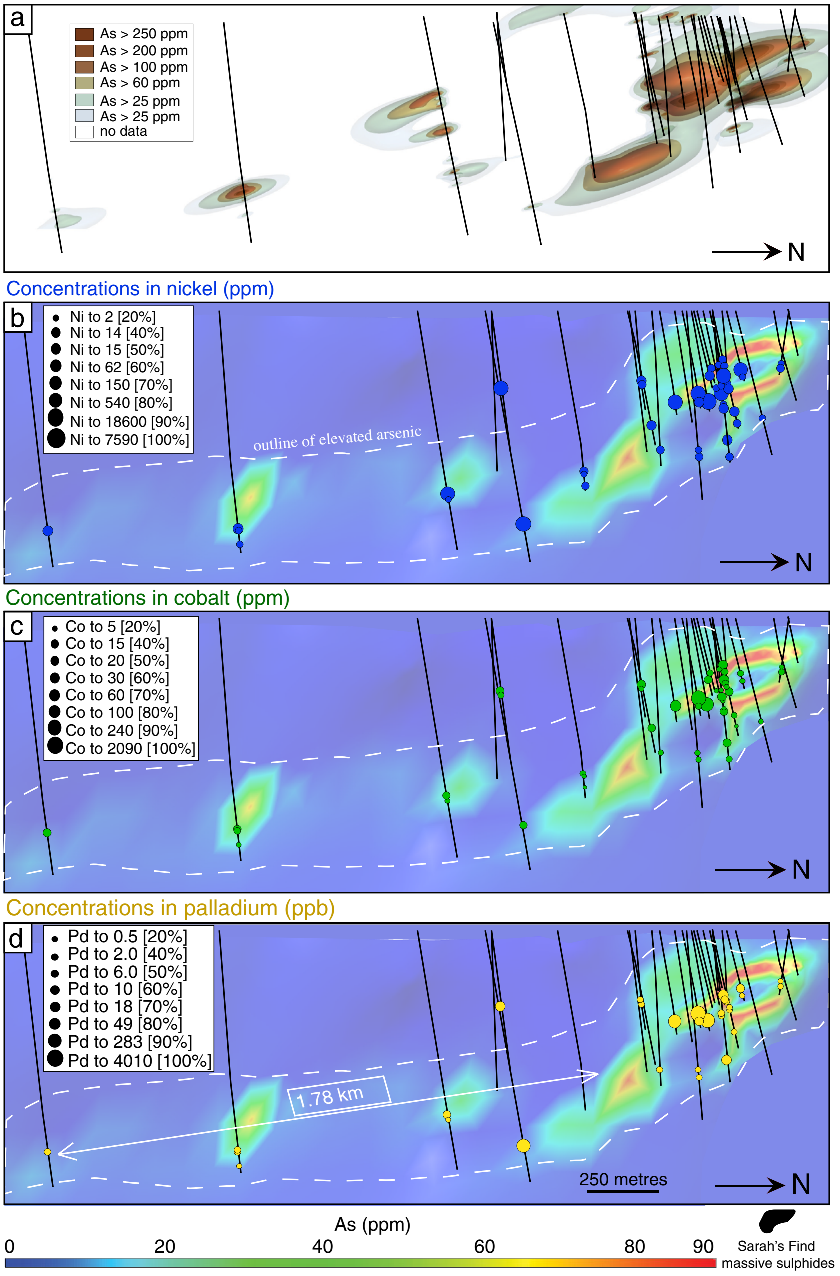

Fig. 17 3D visualisation of concentrations in As (**a**), Ni (**b**), Co (**c**) and Pd (**d**) of all analysed samples, combined with a colour representation of the arsenic concentrations along the footwall contact between the Mount Keith komatiites and the Mount Keith dacite

this Ni-Co-Pd-As halo seems to be very localised close to the footwall contact, which represents a dominant shear zone, and possibly the main pathway for the arsenic-bearing hydrothermal fluids. Importantly, a low As and Ni-Co signal should be considered as neutral, on the grounds that Ni hydrothermal remobilisation is only observed within zones of arsenic enrichment. Understanding the regional and local structural, metamorphic and hydrothermal overprint is crucial.

The distance over which the geochemical halo can be traced seems to differ for pXRF and laboratory XRF, depending on the deposit studied. This difference can be attributed to variations in analysed volumes, to the distribution of the sulphides and arsenides in the rock, and to the in sensitivities of the two instruments. At the Miitel deposit, Widgiemooltha Dome, Western Australia, hydrothermally remobilised nickel arsenides are concentrated within small veins which give rise to very anomalous NiAs signals when analysed by pXRF, but which give diluted signal when sent as meter-long samples to the laboratory (Le Vaillant et al. 2015). At Sarah's Find, the nickel arsenides are dispersed throughout the rock within the foliation; therefore, it is difficult to pick an anomalous NiAs signal with pXRF which only analyses a very small volume of rock, whereas laboratory analyses will pick up all of the nickel arsenides present within the sample. At Sarah's Find, laboratory analyses were able to detect the Ni-Co-Pd-As anomaly farther away from the massive sulphides (over 1500 m),

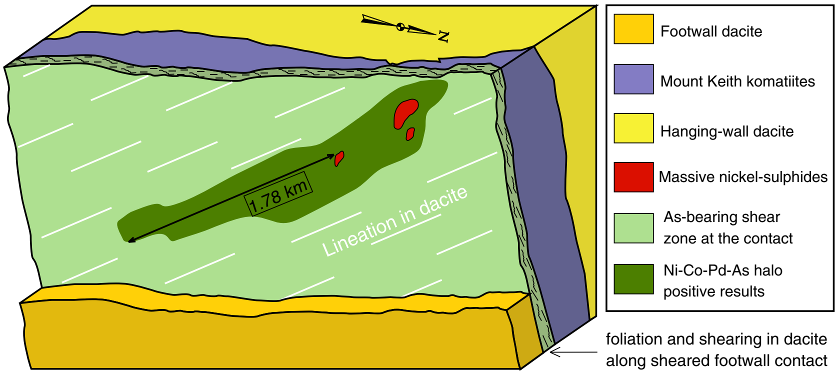

Fig. 18 Interpretative model of the geochemical halo observed around the Sarah's Find ore body

whereas pXRF served as an efficient tool to detect the Ni-As halo when located at a relatively small distance to the massive sulphides (less than 80 m) where nickel arsenides were more concentrated and associated with mechanically sheared sulphides.

Conclusion

A Ni-Co-Pd-As geochemical halo is present around massive nickel sulphides at the Sarah's Find nickel deposit. This halo is interpreted as being the result of physical remobilisation (solid state) and hydrothermal remobilisation of nickel, cobalt and PGE from the massive sulphides. A block diagram synthesizing spatial information and presenting the interpreted shape of this geochemical halo is presented in Fig. 18. Physical remobilisation of the massive sulphides is observed up to 100–150 m away from the massive sulphides within the footwall dacite, along the contact with the Mount Keith Ultramafic Unit, parallel to the direction of shearing. Nickel, cobalt and PGE (mainly Pd and little Pt) are interpreted as being hydrothermally remobilised by syn-deformation As-rich hydrothermal fluids. These As-rich fluids, likely related to a regional orogenic gold event, collected Ni, Co and Pd from the Sarah's Find massive sulphides and redeposited them as gersdorffites within the sheared footwall dacite, along the dominant NNW striking foliation, creating a geochemical halo extending along the direction of shearing up to 1780 m away from the massive sulphides. The extent of this Ni-Co-Pd-As halo is larger than any geochemical tool currently used for nickel sulphide exploration targeting. A geochemical halo similar to the one described in this paper was observed around the Miitel deposits (Le Vaillant et al. 2015) and could potentially exist around any type of magmatic nickel sulphide that has undergone of arsenic metasomatism.

Acknowledgments Financial support for this research was provided by MERIWA (project #M413), BHP Billiton Nickel West, Mincor Resources NL and First Quantum Minerals Ltd. Sarah-Jane Barnes and Danny Savard are thanked for their assistance with the use of the Laser Ablation (LA-ICP-MS) facility at the University of Québec in Chicoutimi (UQAC), Canada. The SIRF scholarship of the University of Western Australia and the MERIWA research grant are greatly appreciated. BHP Billiton is acknowledged for providing on-site access and samples. This project is an output from the CSIRO Minerals Resources Flagship. This is contribution 657 from the ARC Centre of Excellence for Core to Crust Fluid Systems (http://www.ccfs.mq.edu.au). This work was initially commenced as part of a BSc honours project at Monash University by Ahmad Saleem, and Ray Cas is thanked for fruitful discussions. Finally, Dr. Belinda Godèl, Dr. Alistair White, Dr. Rolf Romer and Dr. Federica Zaccarini are thanked for their valuable reviews of this manuscript.

References

Archibald DA, Bettenay LF, Binns RA, Groves DI, Gunthorpe RJ (1978) The evolution of Archaean greenstone terranes, Eastern Goldfields province, Western Australia. Precambrian Res 6:147–163

Bailey J, McDonald AM, Lafrance B, Fedorowich JS (2006) Variations in NI content in sheared magmatic sulfide ore at the Thayer Lindsley mine, Sudbury, Ontario. Can Mineral 44:1063–1077

Barley M, Brown SJA, Krapež B, Kositcin N (2008) Physical volcanology and geochemistry of a Late Archaean volcanic arc: Kurnalpi and Gindalbie Terranes, Eastern Goldfields Superterrane, Western Australia. Precambrian Res 161:53–76

Barnes SJ (2006) Komatiites: petrology, volcanology, metamorphism and geochemistry. Soc Econ Geol Spec Publ 13:13–49

Barnes SJ, Fiorentini ML (2012a) Komatiite magmas and sulfide nickel deposits: a comparison of variably endowed Archean terranes. Econ Geol 107:755–780

Barnes SJ, Liu W (2012b) Pt and Pd mobility in hydrothermal fluids: evidence from komatiites and from thermodynamic modelling. Ore Geology Reviews 44:49–58

Barnes SJ, Van-Kranendonk MJ (2014) Archean andesites in the east Yilgarn craton, Australia: products of plume-crust interaction? Lithosphere 6:80–92

Barnes SJ, Gole MJ, Hill RET (1988) The Agnew nickel deposit, Western Australia: Part II. Sulfide geochemistry, with emphasis on the platinum-group elements. Econ Geol 83:537–550

Barnes SJ, Lesher CM, Sproule RA (2007) Geochemistry of komatiites in the Eastern Goldfields Superterrane, Western Australia and the Abitibi Greenstone Belt, Canada, and implications for the distribution of associated Ni–Cu–PGE deposits. Appl Earth Sci IMM Trans Sect B 116:167–187. doi:10.1179/174327507x271996

Barnes SJ, Fiorentini ML, Duuring P, Grguric BA, Perring CS (2011) The Perseverance and Mount Keith Ni deposits of the Agnew-Wiluna Belt, Yilgarn Craton, Western Australia. Rev Econ Geol 17:51–88

Barrett FM, Binns RA, Groves DI, Marston RJ, McQueen KG (1977) Structural history and metamorphic modification of Archean volcanic-type nickel deposits, Yilgarn Block, Western Australia. Econ Geol 72:1195–1223

Barrie CT, Samson I, Price M, Alvarez BC, Fryer B (2007) Chemical and mineralogical halos around magmatic sulfide deposits CAMIRO Project 04E01. Canadian Mining Industry Research Organization / Organisation Canadienne de recherche sur l'industrie miniere

Bleeker W (1990) Evolution of the Thompson nickel belt and its nickel deposits, Manitoba, Canada. University of New Brunswick, Fredericton, New Brunswick, p 444

Blewett RS, Czarnota K, Henson PA (2010) Structural-event framework for the eastern Yilgarn Craton, Western Australia, and its implications for orogenic gold. Precambrian Res 183:203–229. doi:10.1016/j.precamres.2010.04.004

Boyle RW, Jonasson IR (1973) The geochemistry of arsenic and its use as an indicator element in geochemical prospecting. J Geochem Explor 2:251–296

Brand NW (1993) Sarah's Find: lithogeochemistry of the section 40350MV internal report (unpublished). WMC resources Ltd

Burt DRL, Sheppy NR (eds) (1975) Mount Keith nickel sulfide deposit. Australasian Institute of Mining and Metallurgy

Campbell IH, Naldrett AJ (1979) The influence of silicate:sulfide ratios on the geochemistry of magmatic sulfides. Econ Geol Bull Soc Econ Geol 74:1503–1506

Cassidy KF, Champion DC, Krapez B, Barley ME, Brown SJA, Blewett RS, Groenewald PBg, Tyler IM (2006) A revised geological framework for the Yilgarn Craton, Western Australia In: Resources IA (ed) Western Australia Geological Survey, p 8

Collins JE, Hagemann SG, McCuaig TC, Frost KM (2012) Structural Controls on Sulfide Mobilization at the High-Grade Flying Fox Ni-Cu-PGE Sulfide Deposit, Forrestania Greenstone Belt, Western Australia. Econ Geol 107:1433–1455

Cowden A, Archibald NJ (1987) Massive-sulfide fabrics at Kambalda and their relevance to the inferred stability of monosulfide solid-solution. Can Mineral 25:37–50

Cowden A, Roberts DE (1990) Komatiite hosted nickel sulphide deposits, Kambalda. In: Hughes FE (ed) Economic Geology of Australia and Papua New Guinea. Australian Institute of Mining and Metalurgy, Melbourne, pp 567–581

Donaldson MJ (1981) Redistribution of ore elements during serpentinization and talc-carbonate alteration of some Archean dunites, Western Australia. Econ Geol Bull Soc Econ Geol 76:1698–1713

Dowling SE, Hill RET (1990) Rivers of fire: the physical volacnology of komatiites in the Mount Keith region, Norseman-Wiluna Greenstone Belt, Western Australia Exploration Geoscience Restricted Report 103R:170. CSIRO

Duuring P, Bleeker W, Beresford SW (2007) Structural Modification of the Komatiite-Associated Harmony Nickel Sulfide Deposit, Leinster, Western Australia. Econ Geol 102:277–297

Duuring P, Bleeker W, Beresford SW, Hayward N (2010) Towards a volcanic–structural balance: relative importance of volcanism, folding, and remobilisation of nickel sulphides at the Perseverance Ni–Cu–(PGE) deposit, Western Australia. Mineral Deposita 45:281–311. doi:10.1007/s00126-009-0274-y

Duuring P, Bleeker W, Beresford SW, Fiorentini ML, Rosengren NM (2012) Structural evolution of the Agnew–Wiluna greenstone belt, Eastern Yilgarn Craton and implications for komatiite-hosted Ni sulfide exploration. Aust J Earth Sci 59:765–791. doi:10.1080/08120099.2012.693540

Eisenlohr B (1988) The structural development and controls on mineralisation of the northern sector of the Norseman-Wiluna Belt, Western Australia. University of Western Australia, Perth

Findlay D (1998) Boudinage on radial fractures: an alternative to magmatic models for the emplacement of nickel ores, Lunnon Shoot, Kambalda, Western Australia. Aust J Earth Sci 45:943–954

Fiorentini ML, Rosengren N, Beresford SW, Grguric B, Barley ME (2007) Controls on the emplacement and genesis of the MKD5 and Sarah's Find Ni–Cu–PGE deposits, Mount Keith, Agnew–Wiluna Greenstone Belt, Western Australia. Mineral Deposita 42:847–877. doi:10.1007/s00126-007-0140-8

Fiorentini ML, Barnes SJ, Maier WD, Burnham OM, Heggie G (2010a) Global Variability in the Platinum-group Element Contents of Komatiites. J Petrol 52:83–112. doi:10.1093/petrology/egq074

Fiorentini ML, Beresford SW, Rosengren N, Barley ME, McCuaig TC (2010b) Contrasting komatiite belts, associated Ni–Cu–(PGE) deposit styles and assimilation histories. Aust J Earth Sci 57:543–566. doi:10.1080/08120099.2010.492911

Gole MJ, Robertson J, Barnes SJ (2013) Extrusive Origin and Structural Modification of the Komatiitic Mount Keith Ultramafic Unit. Econ Geol Bull Soc Econ Geol 108:1731–1752

Goscombe B, Blewett RS, Czarnota K, Groenewald PB, Mass R (2009) Metamorphic evolution and integrated terrane anlysis of the Eastern Yilgarn Craton; rationale, methods, outcomes and interpretation. Geosci Aust Rec 2009(23):1–270

Groves DI, Goldfarb RJ, Robert F, Hart CJR (2003) Gold deposits in metamorphic belts: overview of current understanding, outstanding problems, future research, and exploration significance. Econ Geol Bull Soc Econ Geol 98:1–29

Hallberg JA (1984) A geochemical aid to igneous rock type identification in deeply weathered terrain. J Geochem Explor 20:1–8

Hammond RL, Nisbet BW (1992) Towards a structural and tectonic framework for the Norseman-Wiluna Greenstone Belt, Western Australia In: Glover JE, Ho SE (eds) The Archaean: Terrains, Processes and Metallogeny. University of Western Australia, Geol department and University, pp 39–50

Hanley JJ, Bray CJ (2009) The trace metal content of amphibole as proximity indicator for Cu-Ni-PGE mineralization in the footwall of the Sudbury igneous complex, Ontario, Canada. Econ Geol 104:113–125

Hayward N (2004) Structural geology of the Mt Keith Mine area. WMC Resources Ltd., internal report, (unpublished)

Heath C, Lahaye Y, Stone WE, Lambert D (2001) Origin of variations in nickel tenor along the strike of the Edwards lode nickel sulfide orebody, Kambalda, Western Australia. Can Mineral 39:655–671

Hedenquist JW, Thompson JFH, Goldfarb RJ, Richards JP (2005) 100th Anniversary Volume. Econ Geol 1133

Hill RET, Barnes SJ, Gole MJ, Dowling SE (1995) The volcanology of komatiites as deduced from field relationships in the Norseman-Wiluna greenstone belt, Western Australia. Lithos 34:159–188

Hronsky J, Schodde RC (2006) Nickel exploration history of the Yilgarn Craton: from the nickel boom to today. Soc Econ Geol Spec Publ 13:1–11

Ketris MP, Yudovich Y (2009) Estimations of clarkes for carbonaceous biolithes: world averages for trace element contents in black shales and coals. Int J Coal Geol 78:135–148

Klemm DD (1965) Synthesen und Analysen in den Drejeckdiagrammen FeAsS-CoAsS-NiAsS und FeS2-CoS2-NiS2: Neues Jahrbuch für Mineralogie. Abhandlungen 103:205–255

Large RR, Bull SW, Maslennikov VV (2011) A Carbonaceous Sedimentary Source-Rock Model for Carlin-Type and Orogenic Gold Deposits. Econ Geol 106:331–358

Layton-Matthews D, Lesher CM, Burnham OM, Liwanag J, Halden NM, Hulbert L, Peck DC (2007) Magmatic Ni-Cu-platinum-group element deposits of the thomson nickel belt. In: Goodfellow WD (ed) Mineral deposits of Canada: a synthethis of major deposit-types, district metallogeny, the evolution of geological provinces, and exploration methods. pp 409–432

Le Vaillant M, Barnes SJ, Fisher L, Fiorentini ML, Caruso S (2014) Use and calibration of portable X-Ray fluorescence analysers: application to lithogeochemical exploration for komatiite-hosted nickel sulphide deposits. Geochem Explor Environ Anal 14:199–209. doi:10.1144/geochem2012-166

Le Vaillant M, Barnes SJ, Fiorentini ML, Miller J, McCuaig TC, Muccilli P (2015) A Hydrothermal Ni-As-PGE Geochemical Halo Around the Miitel Komatiite-Hosted Nickel Sulfide Deposit, Yilgarn Craton, Western Australia. Econ Geol 110:505–530. doi:10.2113/econgeo.110.2.505

Platt JP, Allchurch PD, Rutland RR (1978) Archaean tectonics in the Agnew supracrustal belt, Western Australia. Precambrian Res 7:3–30

Quinby-Hunt MS, Wide P, Berry WBN (1989) Element geochemistry of low-calcic black shales - statistical comparison with other shales. US Geol Surv Circ 1037:8–15

Rosengren NM (2004) Architecture and emplacement origin of an Archaean Komatiitic Dunite and Associated Ni-sulfide mineralisation: Mout Keith, Agnew-Wiluna Greenstone Belt, Yilgarn Craton, Western Australia. Unpublished PhD Thesis. Monash University

Rosengren NM, Beresford SW, Grguric BA, Cas RAF (2005) An intrusive origin for the komatiitic dunite-hosted mount Keith disseminated nickel sulfide deposit, Western Australia. Econ Geol Bull Soc Econ Geol 100:149–156

Rosengren NM, Grguric BA, Beresford SW, Fiorentini ML, Cas RAF (2007) Internal stratigraphic architecture of the komatiitic dunite-hosted MKD5 disseminated nickel sulfide deposit, Mount Keith Domain, Agnew-Wiluna Greenstone Belt, Western Australia. Mineral Deposita 42:821–845. doi:10.1007/s00126-007-0139-1

Rosengren NM, Cas RAF, Beresford SW, Palich BM (2008) Reconstruction of an extensive Archaean dacitic submarine volcanic complex associated with the komatiite-hosted Mt Keith nickel deposit, Agnew-Wiluna Greenstone Belt, Yilgarn Craton, Western Australia. Precambrian Res 161:34–52

Seat Z, Stone WE, Mapleson DB, Daddow BC (2004) Tenor variation within komatiite-associated nickel sulphide deposits: insights from the Wannaway Deposit, Widgiemooltha Dome, Western Australia. Mineral Petrol 82:317–339. doi:10.1007/s00710-004-0047-3

Swager CP (1997) Tectono-stratigraphy of the late Archaean greenstone terranes in the southern Eastern Goldfields, Western Australia. Precambrian Res 83:11–42

Vukmanovic Z, Reddy SM, Godel B, Barnes SJ, Fiorentini ML, Barnes S-J, Kilburn MR (2014) Relationship between microstructures and grain-scale trace element distribution in komatiite-hosted magmatic sulphide ores. Lithos 184–187:42–61. doi:10.1016/j.lithos.2013.10.037

Williams PR, Whitaker AJ (1993) Gneiss domes and extensional deformation in the highly mineralised Archaean Eastern Goldfields Province, Western Australia. Ore Geol Rev 8:141–162